DEPARTMENT OF
MATERIALS SCIENCE AND ENGINEERING

Stereology applied to GBCD

Texture, Microstructure & Anisotropy

A.D. Rollett

Last revised: 19th Mar. '14

Objectives

- To instruct in methods of *measuring* characteristics of microstructure: grain size, shape, orientation; phase structure; grain boundary length, curvature etc.

- To describe methods of obtaining 3D information from 2D cross-sections: *stereology.*

- To show how to obtain useful microstructural quantities from plane sections through microstructures.

- In particular, to show how to apply stereology to the problem of measuring 5-parameter Grain Boundary Character Distributions (GBCD) without having to perform serial sectioning.

Objectives   Notation   Equations   Delesse S_V-P_L L_A-P_L Topology   Grain_Size   Distributions

Stereology: References

- These slides are partly based on: *Quantitative Stereology*, E.E. Underwood, Addison-Wesley, 1970.
  - equation numbers given where appropriate.
- Also useful: M.G. Kendall & P.A.P. Moran, *Geometrical Probability*, Griffin (1963).
- Kim C S and Rohrer G S Geometric and crystallographic characterization of WC surfaces and grain boundaries in WC-Co composites. *Interface Science*, **12** 19-27 (2004).
- C.-S. Kim, Y. Hu, G.S. Rohrer, V. Randle, "Five-Parameter Grain Boundary Distribution in Grain Boundary Engineered Brass," *Scripta Materialia*, **52** (2005) 633-637.
- Miller HM, Saylor DM, Dasher BSE, Rollett AD, Rohrer GS. Crystallographic Distribution of Internal Interfaces in Spinel Polycrystals. *Materials Science Forum* **467-470**:783 (2004).
- Rohrer GS, Saylor DM, El Dasher B, Adams BL, Rollett AD, Wynblatt P. The distribution of internal interfaces in polycrystals. *Z. Metall*. 2004; **95**:197.
- Saylor DM, El Dasher B, Pang Y, Miller HM, Wynblatt P, Rollett AD, Rohrer GS. Habits of grains in dense polycrystalline solids. *Journal of The American Ceramic Society* 2004; **87**:724.
- Saylor DM, El Dasher BS, Rollett AD, Rohrer GS. Distribution of grain boundaries in aluminum as a function of five macroscopic parameters. *Acta mater*. 2004; **52**:3649.
- Saylor DM, El-Dasher BS, Adams BL, Rohrer GS. Measuring the Five Parameter Grain Boundary Distribution From Observations of Planar Sections. *Metall. Mater. Trans.* 2004; **35A**:1981.
- Saylor DM, Morawiec A, Rohrer GS. Distribution and Energies of Grain Boundaries as a Function of Five Degrees of Freedom. *Journal of The American Ceramic Society* 2002; **85**:3081.
- Saylor DM, Morawiec A, Rohrer GS. Distribution of Grain Boundaries in Magnesia as a Function of Five Macroscopic Parameters. *Acta mater*. 2003; **51**:3663.
- Saylor DM, Rohrer GS. Determining Crystal Habits from Observations of Planar Sections. *Journal of The American Ceramic Society* 2002; **85**:2799.

Objectives **Notation** **Equations** **Delesse** $\mathbf{S_V}$-$\mathbf{P_L}$ $\mathbf{L_A}$-$\mathbf{P_L}$ **Topology** **Grain_Size** **Distributions**

Questions

1. What is the connection between lines/traces observed on planar cross-sections of 3D interfaces and surface area?

2. How does Buffon's Needle measure π?

3. What is the definition of Stereology?

4. What are some examples of measureable quantities and derived quantities in stereology?

5. What is an accumulator diagram/ stereogram?

6. When we observe the trace of a boundary/interface in a cross-section, what can we infer about the true normal to that interface?

7. How do we use the trace, once converted to crystal coordinates, in an accumulator stereogram?

- What is the standard discretization of the (hemi-) spherical accumulator stereogram?

- Why do we divide up the declination (co-latitude) angle in increments of $\cos(\theta)$?

- What is the key difference between analyzing surface normals and grain boundaries (to get the GBCD)?

- Given a 3D microstructure (i.e. image as an orientation map), what is the best way to proceed to extract grain boundary normals (and misorientations)?

- What units do we (typically) use for GBCD and Misorientation Distributions?

Measurable Quantities

- N := <u>n</u>umber (e.g. of points, intersections)
- P := <u>p</u>oints
- L := <u>l</u>ine length
- *Blue* $\Rightarrow$ easily measured directly from images
- A := <u>a</u>rea
- S := <u>s</u>urface or interface area
- V := <u>v</u>olume
- *Red* $\Rightarrow$ not easily measured directly

Objectives   Notation   Equations   Delesse S_V-P_L L_A-P_L Topology   Grain_Size   Distributions

Definitions

Subscripts:

P := per test point

L := per unit of line

A := per unit area

V := per unit volume

T := total

overbar:= average

<x> = average of x

E.g. P_A :=

Points per unit area

TABLE 1.1

List of basic symbols and their definitions

Symbol	Dimensions*	Definition
P		Number of point elements, or test points
P_P		Point fraction. Number of points (in areal features) per test point
P_L	mm^{-1}	Number of point intersections per unit length of test line
P_A	mm^{-2}	Number of points per unit test area
P_V	mm^{-3}	Number of points per unit test volume
L	mm	Length of lineal elements, or test line length
L_L	mm/mm	Lineal fraction. Length of lineal intercepts per unit length of test line
L_A	mm/mm^2	Length of lineal elements per unit test area
L_V	mm/mm^3	Length of lineal elements per unit test volume
A	mm^2	Planar area of intercepted features, or test area
S	mm^2	Surface or interface area (not necessarily planar)
A_A	mm^2/mm^2	Area fraction. Area of intercepted features per unit test area
S_V	mm^2/mm^3	Surface area per unit test volume
V	mm^3	Volume of three-dimensional features, or test volume
V_V	mm^3/mm^3	Volume fraction. Volume of features per unit test volume
N		Number of features (as opposed to points)
N_L	mm^{-1}	Number of interceptions of features per unit length of test line
N_A	mm^{-2}	Number of interceptions of features per unit test area
N_V	mm^{-3}	Number of features per unit test volume
$\bar{L}$	mm	Average lineal intercept, L_L/N_L
$\bar{A}$	mm^2	Average areal intercept, A_A/N_A
$\bar{S}$	mm^2	Average surface area, S_V/N_V
$\bar{V}$	mm^3	Average volume, V_V/N_V

*Arbitrarily shown in millimeters.

[Underwood]

Objectives   Notation   Equations   Delesse S_V-P_L L_A-P_L Topology   Grain_Size   Distributions

Relationships between Quantities

- $V_V = A_A = L_L = P_P$ mm^0
- $S_V = (4/\pi)L_A = 2P_L$ mm^{-1}
- $L_V = 2P_A$ mm^{-2}
- $P_V = 0.5L_V S_V = 2P_A P_L$ mm^{-3} (2.1-4).
- These are exact relationships, provided that measurements are made with statistical uniformity (randomly). Obviously experimental data is subject to error.
- Notation and Eq. numbers from Underwood, 1971

Objectives   Notation   Equations Delesse S_V-P_L L_A-P_L Topology Grain_Size Distributions

Relationships between Quantities

TABLE 2.1

Relationship of measured (○) to calculated (□) quantities

Microstructural feature	Dimensions of symbols (arbitrarily expressed in terms of millimeters)			
	mm^0	mm^{-1}	mm^{-2}	mm^{-3}
Points	P_P	P_L →	P_A →	P_V
Lines	L_L	L_A	L_V	—
Surfaces	A_A	S_V	—	—
Volumes	V_V	—	—	—

Remember that it is not easy to obtain true 3D measurements (squares) and so we must find stereological methods to estimate the 3D quantities (squares) from 2D measurements (circles).

Objectives   Notation   Equations   Delesse S_V-P_L L_A-P_L Topology   Grain_Size   Distributions

Surface Area (per unit volume)

- $S_V = 2P_L$ (2.2).

- Derivation based on random intersection of lines with (internal) surfaces. Probability of intersection depends on inclination angle, θ. Averaging θ gives factor of 2.

- Clearly, the area of grain boundary per unit volume is measured by S_V.

Objectives   Notation   Equations   Delesse S_V-P_L L_A-P_L Topology   Grain_Size   Distributions
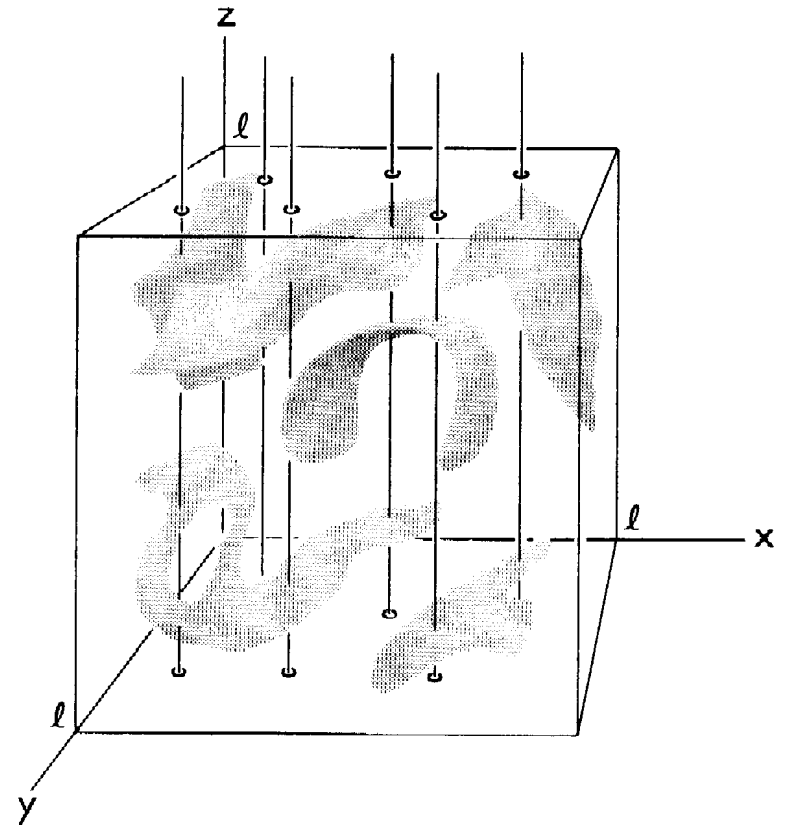
$$S_V = 2P_L$$
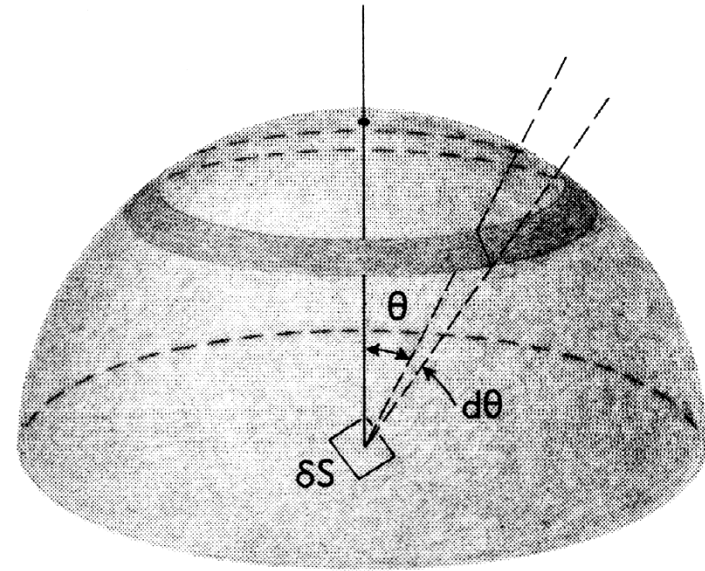
- Derivation based on uniform distribution of elementary areas.
- Consider the dA to be distributed over the surface of a sphere. The sphere represents the effect of randomly (uniformly) distributed surfaces.
- Projected area = $dA \cos\theta$.
- Probability that a *vertical* line will intersect with a given patch of area on the sphere is proportional to *projected* area of that patch onto the horizontal plane.
- Therefore we integrate both the projected area and the total area of the hemisphere, and take the ratio of the two quantities

Objectives   Notation   Equations   Delesse S_V-P_L L_A-P_L Topology   Grain_Size   Distributions

$$S_V = 2P_L$$

$$dA = r^2 \sin\theta\, d\theta\, d\varphi; \qquad dA_{projected} = dA\cos\theta$$

$$\frac{\langle A_{projected}\rangle}{A_{total}} = \frac{\iint dA\cos\theta}{\iint dA}$$

$$\frac{\langle A_{projected}\rangle}{A_{total}} = \frac{\int_0^{2\pi}\int_0^{\pi/2} r^2 \sin\theta\cos\theta\, d\theta\, d\varphi}{\int_0^{2\pi}\int_0^{\pi/2} r^2 \sin\theta\, d\theta\, d\varphi} = \frac{0.5\int_0^{\pi/2}\sin 2\theta\, d\theta}{\int_0^{\pi/2}\sin\theta\, d\theta}$$

$$\frac{\langle A_{projected}\rangle}{A_{total}} = \frac{1/4\left[-\cos 2\theta\right]_0^{\pi/2}}{\left[\cos\theta\right]_0^{\pi/2}} = \frac{1/4\left[1-(-1)\right]}{1} = \frac{2}{4}$$

$$\frac{\langle A_{projected}\rangle}{A_{total}} = \frac{1}{2} = \frac{P_L}{S_V}$$

Objectives   Notation   Equations   Delesse S_V-P_L L_A-P_L Topology   Grain_Size   Distributions

Length of Line per Unit Area, L_A versus Intersection Points Density, P_L

- Set up the problem with a set of test lines (vertical, arbitrarily) and a line to be sampled. The sample line can lie at any angle: what will we measure?
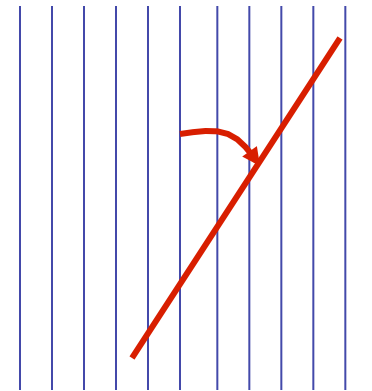
ref: p38/39 in Underwood

This was first considered by Buffon, *Essai d'arithmetique morale*, Supplément à l'Histoire Naturelle, **4**, (1777) and the method has been used to estimate the value of π. Consequently, this procedure is also known as Buffon's Needle.

Objectives   Notation   Equations   Delesse S_V-P_L L_A-P_L Topology   Grain_Size   Distributions

$L_A = \pi/2\ P_L,\ contd.$

Δx, *or d*

l

θ

$l \cos \theta$

$l \sin \theta$
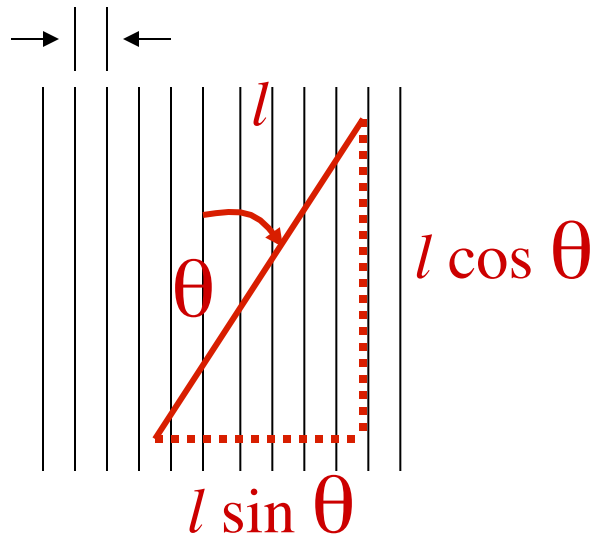
The number of points of intersection with the test grid depends on the angle between the sample line and the grid. Larger θ value means more intersections. The projected length = $l \sin \theta = l\ P_L\ \Delta x$.

$$P_L = \frac{\sin\theta}{\Delta x}$$

• Line length in area, L_A; consider an arbitrary area of x by x :

$$L_A = x\frac{x}{\Delta x} \div \frac{1}{x^2} = \frac{1}{\Delta x}$$

Therefore to find the relationship between P_L and L_A for the general case where we do not know Δx, we must average over all values of the angle θ.

Objectives   Notation   Equations   Delesse S_V-P_L L_A-P_L Topology   Grain_Size   Distributions

$L_A = \pi/2\,P_L$, contd.

- Probability of intersection with test line given by average over all values of θ:

$$p = \frac{\int_0^\pi l\sin\theta\,d\theta}{\int_0^\pi l\,d\theta} = \frac{l}{l}\frac{\left[-\cos\theta\right]_0^\pi}{\left[\theta\right]_0^\pi} = \frac{2}{\pi}$$

θ

- Density of intersection points, P_L, to Line Density per unit area, L_A, is given by this probability. Note that a simple experiment estimates π (but beware of errors!).
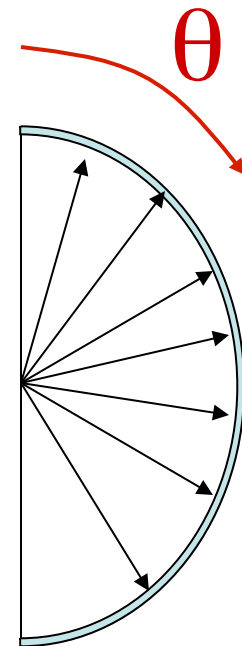
Buffon's Needle Experiment

- In fact, to perform an actual experiment by dropping a needle onto paper requires care. One must always perform a very large number of trials in order to obtain an accurate value. The best approach is to use ruled paper with parallel lines at a spacing, d, and a needle of length, l, less than (or equal to) the line spacing, $l \le d$. Then one may use the following formula. (A more complicated formula is needed for long needles.) The total number of dropped needles is N and the number that cross (intersect with) a line is n.

$$\pi = \frac{2(l/d)N}{n}$$

See: http://www.ms.uky.edu/~mai/java/stat/buff.html
Also http://mathworld.wolfram.com/BuffonsNeedleProblem.html

Objectives Notation Equations Delesse S_V-P_L L_A-P_L Topology Grain_Size Distributions

$$S_V = (4/\pi)L_A$$

- If we can measure the *line length per unit area, L_A,* directly, then there is an equivalent relationship to the *surface area per unit volume, S_V.*

- This relationship is immediately obtained from the previous equation and a further derivation (not given here) known as *Buffon's Needle*:

$$S_V / 2 = P_L \text{ and } P_L = (2/\pi)\, L_A,$$
which together give:
$$S_V = (4/\pi)\, L_A.$$

- Careful! This simple analysis leads to an elegant experiment which consists of dropping a needle on ruled paper and counting intersections. This is, however, an inefficient way of estimating π.

- In the OIM software, for example, grain boundaries can be automatically recognized based on misorientation and their lengths counted to give an estimate of L_A. From this, the *grain boundary area per unit volume* can be estimated (as S_V).

Objectives   Notation   Equations   Delesse S_V-P_L L_A-P_L Topology   Grain_Size   Distributions

Example Problem: Tungsten Carbide

- Example Problem (Changsoo Kim, Prof. G. Rohrer): consider a composite structure (WC in Co) that contains *faceted particles*. The particles are not joined together although they may touch at certain points. You would like to know how much interfacial area per unit volume the particles have (from which you can obtain the area per particle). Given data on the line length per unit area in sections, you can immediately obtain the surface area per unit volume, *provided that the sections intersect the facets randomly.*

Faceted particles, contd.

- An interesting extension of this problem is as follows. What if each facet belongs to one of a set of crystallographic facet types, and we would like to know how much area each *facet type* has?

- What can we measure, assuming that we have EBSD/OIM maps? In addition to the line lengths of grain boundary, we can also measure the orientation of each line. If the facets are limited to a all number of types, say {100}, {111} and {110}, then it is possible to assign each line to one type (except for a few ambiguous positions). This is true because the grain boundary "line" that you see in a micrograph must be a *tangent* to the boundary plane, which means that it must be perpendicular to the boundary normal. In crystallographic terms, it must lie in the *zone* of the plane normal.

Determining Average 3-D Shape for WC

Problem : Crystals are three-dimensional, micrographs are two-dimensional

Serial sectioning :
- labor intensive, time consuming
- involves inaccuracies in measuring each slice especially in hard materials
3DXDM :
- needs specific equipment,
i.e. a synchrotron!

Do these WC crystals have a common, *crystallographic* shape?

$60 \times 60 \ \mu m^2$
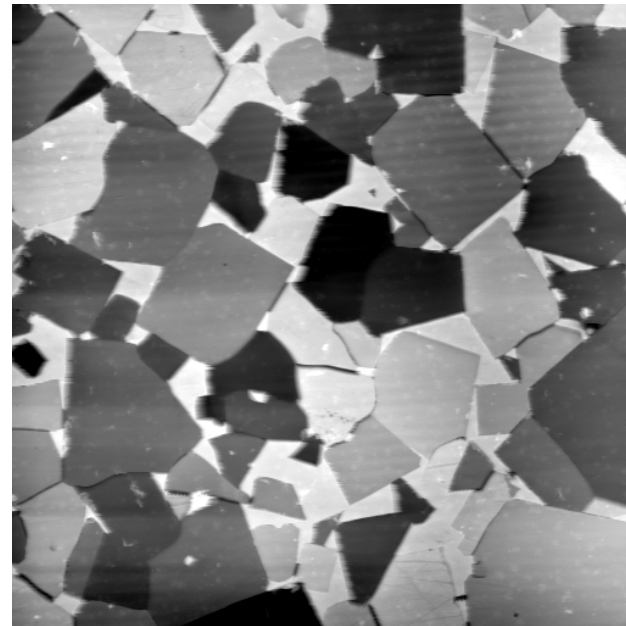
Measurement from Two-Dimensional Sections

We know that each habit plane is in
the zone of the observed surface trace

$\hat{z}$

$\hat{y}$

$\hat{x}$

l_{ij}

l_{12} l_{13} l_{23} l_{24} l_{21}

$i = 1$ $i = 2$

l_{11} l_{22}
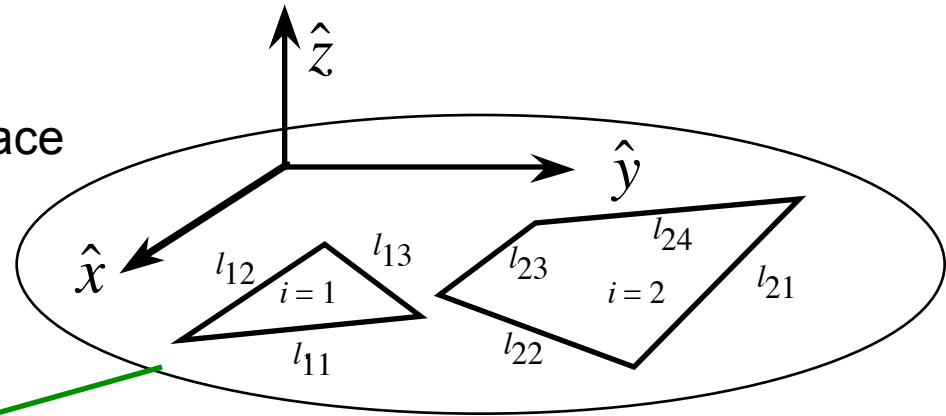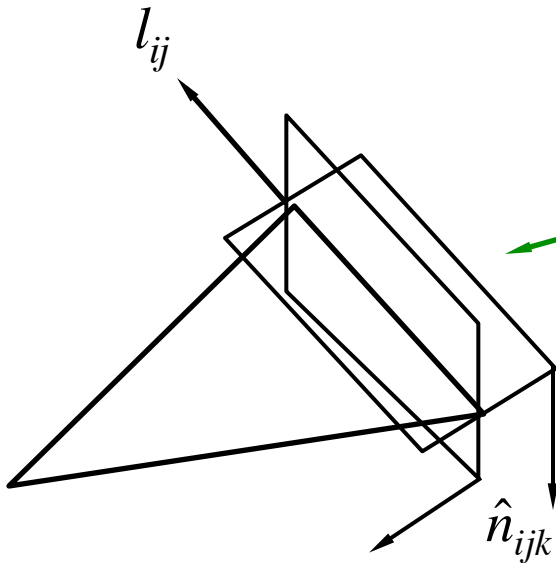
$\hat{n}_{ijk}$

Assumption : Fully faceted isolated
crystalline inclusions dispersed in a
second phase

$\hat{n}_{ijk}$

$$l_{ij} \bullet \hat{n}_{ijk} = 0$$

$\bar{l}_{ij}$ $\hat{y}$

→ For every line segment observed, there is a set of possible planes that contains a
correct habit plane together with a set of incorrect planes that are sampled randomly.
Therefore, after many sets of planes are observed and transformed into the crystal
reference frame, the frequency with which the true habit planes are observed will
greatly exceed the frequency with which non-habit planes are observed.

[Changsoo Kim, 2004]

Notation: l_{ij}: trace of jth facet of the ith particle
n_{ijk}: normal, perpendicular to trace.

Transform Observations to Crystal Frame

Transformation (orientation) matrix from (Bunge) Euler angles:

$$g(\phi_1, \Phi, \phi_2) =$$

$$\begin{bmatrix} c\phi_1 c\phi_2 - s\phi_1 s\phi_2 c\Phi & s\phi_1 c\phi_2 + c\phi_1 s\phi_2 c\Phi & s\phi_2 s\Phi \\ -c\phi_1 s\phi_2 - s\phi_1 c\phi_2 c\Phi & -s\phi_1 s\phi_2 + c\phi_1 c\phi_2 c\Phi & c\phi_2 s\Phi \\ s\phi_1 s\Phi & -c\phi_1 s\Phi & c\Phi \end{bmatrix}$$

c : cosine, s : sine

$$\hat{n}_i^{(crystal)} = g_{ij}(\phi_1, \Phi, \phi_2)\hat{n}_j^{(sample)}$$

25.00 µm = 100 steps   IQ 28.12...104.22, IPF [001]

$100 \times 100 \ \mu m^2$

Vector components in crystal reference frame

Vector components in laboratory reference frame

$10\bar{1}0$

0001 $2\bar{1}\bar{1}0$

[Changsoo Kim, 2004]

Basic Idea

transform to
crystal reference
frame

Trace Pole

Poles of
possible
planes

Observed surface trace

Draw the zone of the Trace Pole:
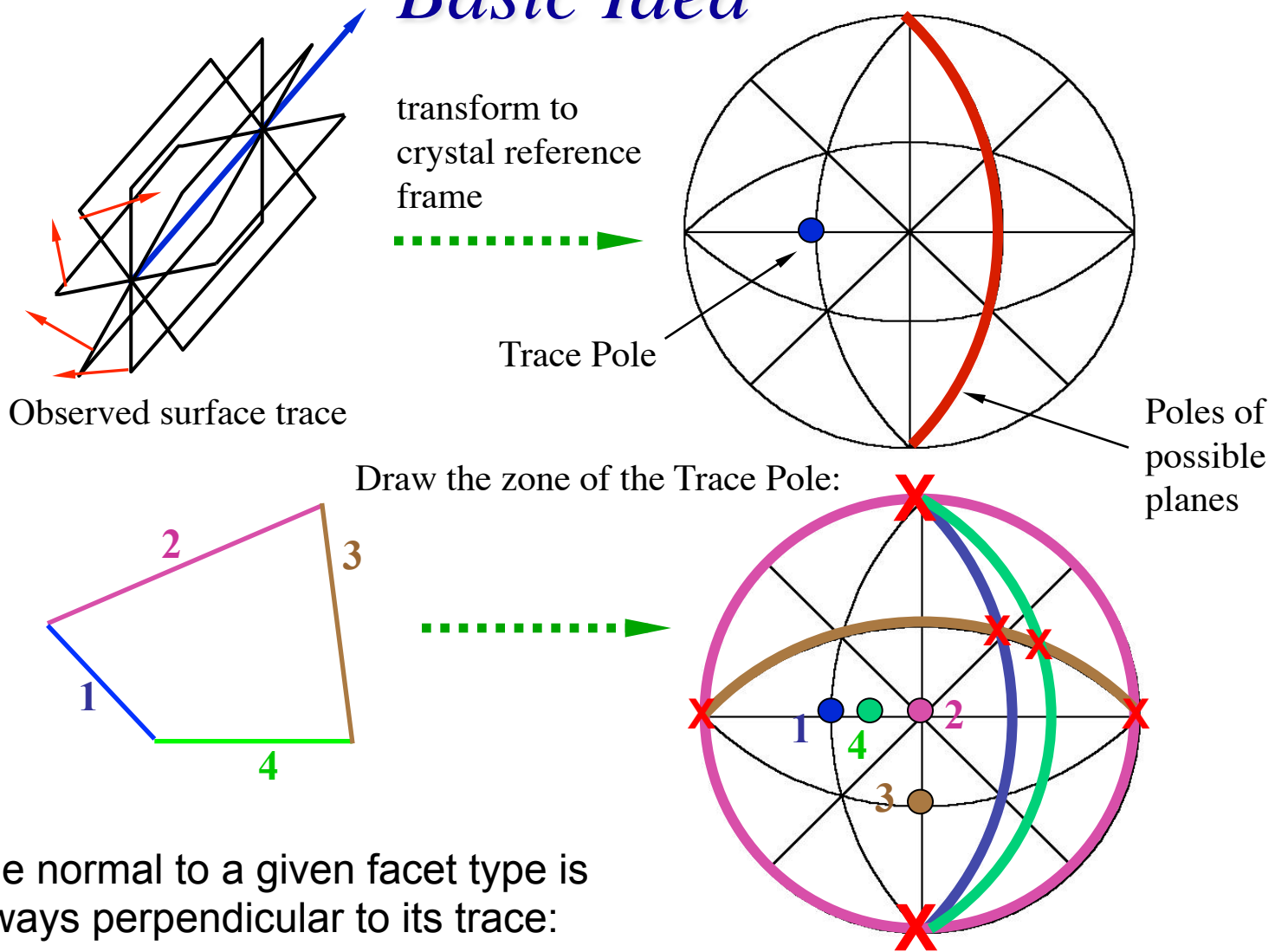
The normal to a given facet type is
always perpendicular to its trace:

[Changsoo Kim, 2004]

Therefore, if we repeat this procedure for many WC
grains, high intensities (peaks) will occur at the positions
of the habit plane normals

Crystallography

Step 1: identify a reference direction.

Step 2: identify a tangent to a grain boundary for a specified segment length of boundary.

Step 3: measure the angle between the g.b. tangent and the reference direction.

Step 4: convert the direction, t_{sample}, in sample coordinates to a direction, $t_{crystal}$, in crystal coordinates, using the crystal orientation, g.

Steps 2-4: *repeat for all boundaries*

Step 5: classify/sort each boundary segment according to the type of grain boundary.

WC in Co, courtesy of Changsoo Kim

t_{sample}

θ
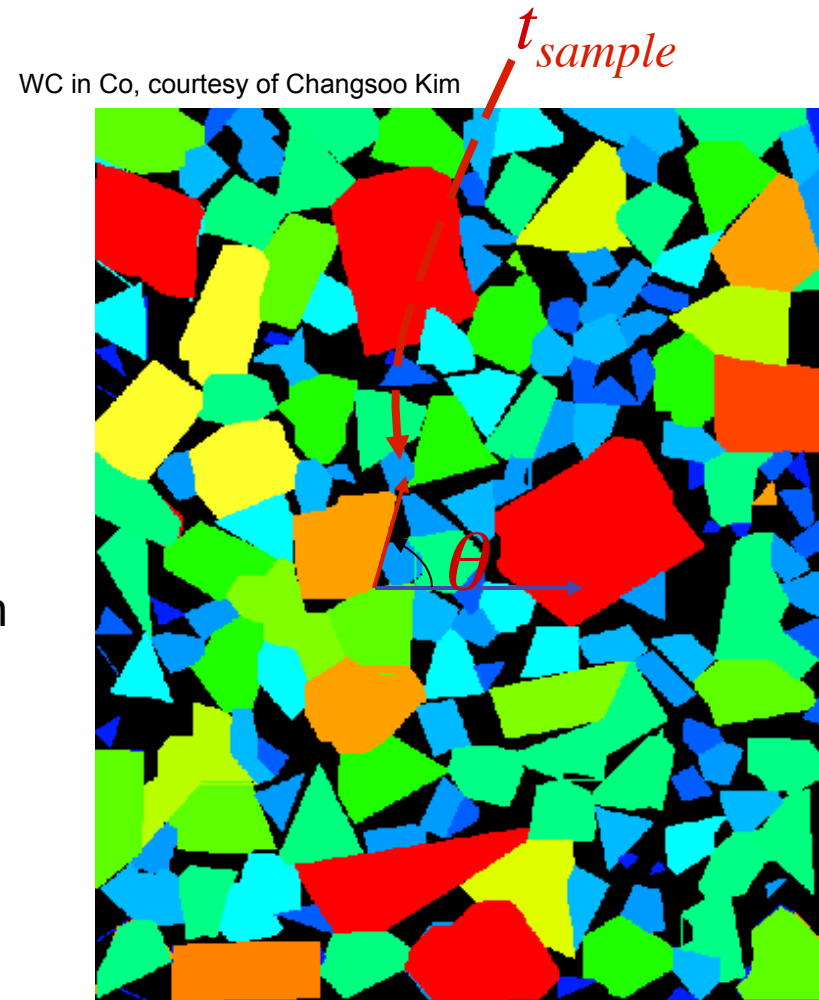
$$t_{crystal} = g \bullet t_{sample}$$

Faceted particles, facet analysis

The set of measured tangents, $\{t_{crystal}\}$ can be plotted on a stereographic projection

Red poles must lie on {110} facets

Blue poles must lie on {100} facets

Discussion: where would you expect to find poles for lines associated with {111} facets?

Faceted particles, area analysis

- The results depicted in the previous slide suggest (assuming equal line lengths for each sample) that the ratio of values is:

$$L_{A/110}: L_{A/100} = 6{:}4$$

$\Rightarrow$ $\quad S_{V/110}: S_{V/100} = 6{:}4$

From these results, it is possible to deduce ratios of interfacial energies.

Habit Probability Function

$\hat{z}$

$\hat{x}$ $\quad l_{12} \quad_{i=1} \quad l_{13} \quad l_{23} \quad_{i=2} \quad l_{24} \quad l_{21}$

$$\vec{p}(\hat{n}') = \frac{\sum_{i,j,k}^{11} g_i \hat{n}_{ijk} \, |l_{ij}^{22}| \sin\theta_k}{\sum_{i,j,k} |l_{ij}| \sin\theta_k}$$

When this probability is plotted as a function of the normal, *n'*, (in the crystal frame) maxima will occur at the habit planes.
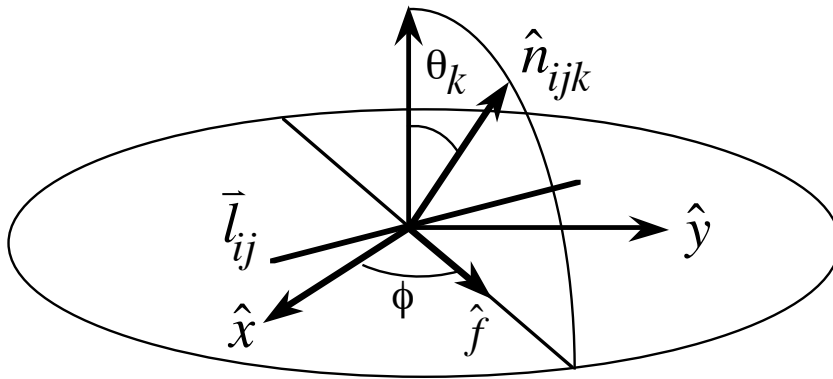
The probability that a plane is observed is proportional to $\sin\theta_k$ and to the line length $|l_{ij}|$. Planes parallel to the section plane are not observed whereas planes perpendicular to the section have the maximum probability of being observed.

3D reconstruction :

The dot product of any l_{ij} with each habit plane vanishes for the habit plane that created the surface trace. Since the total length of a set of randomly distributed lines intersecting an area is proportional to that area, the ratios of the line lengths associated with each plane is an estimate of the relative surface areas.

[Changsoo Kim, 2004]

Numerical Analysis

Discretization $\phi : 0 \sim \pi$

$\cos\theta : 1 \sim -1$

→ Grid discretization in increments of ϕ and $(\cos\theta)$ gives equal area for each cell
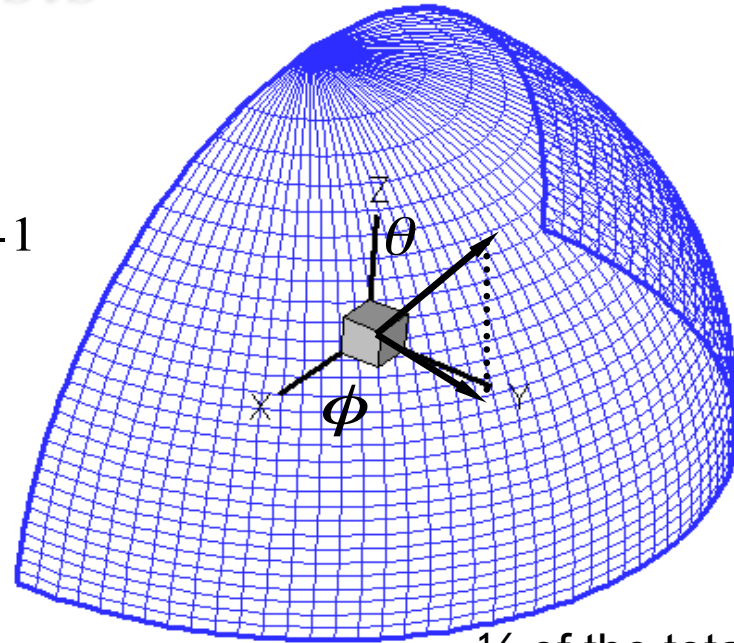
½ of the total grid

Procedure: compute a series of points along the zone of each trace pole and bin them in the crystal frame.

$$\vec{p}(\hat{n}') = \frac{\sum_{i,j,k} g_i \hat{n}_{ijk} \mid l_{ij} \mid \sin\theta_k}{\sum_{i,j,k} \mid l_{ij} \mid \sin\theta_k}$$

Probability function, normalized to give units of: Multiples of Random Distribution (MRD)

[Changsoo Kim, 2004]

1 line segment of 1 grain   +   another line segment of 1 grain   =   2 line segments of 1 grain

another grain

+   + ... =

15 grains

→

30 grains   →   50 grains   →   200 grains
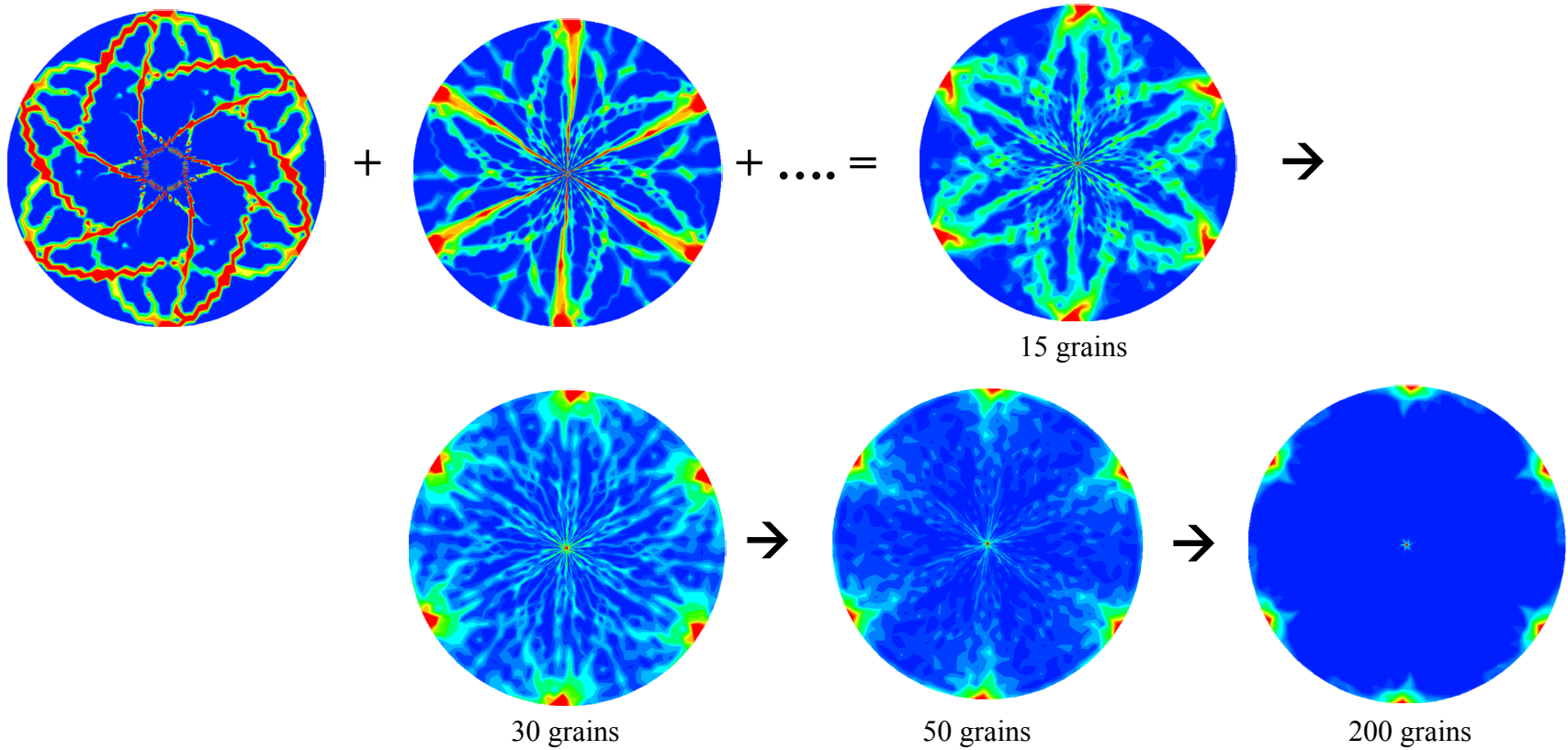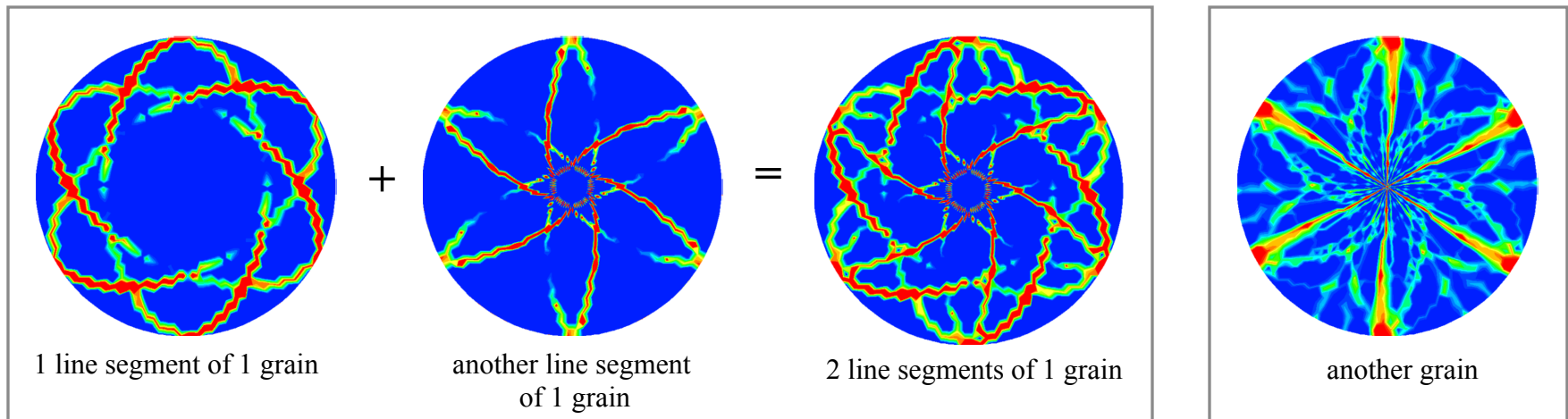
[Changsoo Kim, 2004]

Results

~50 WC grains

~200 WC grains
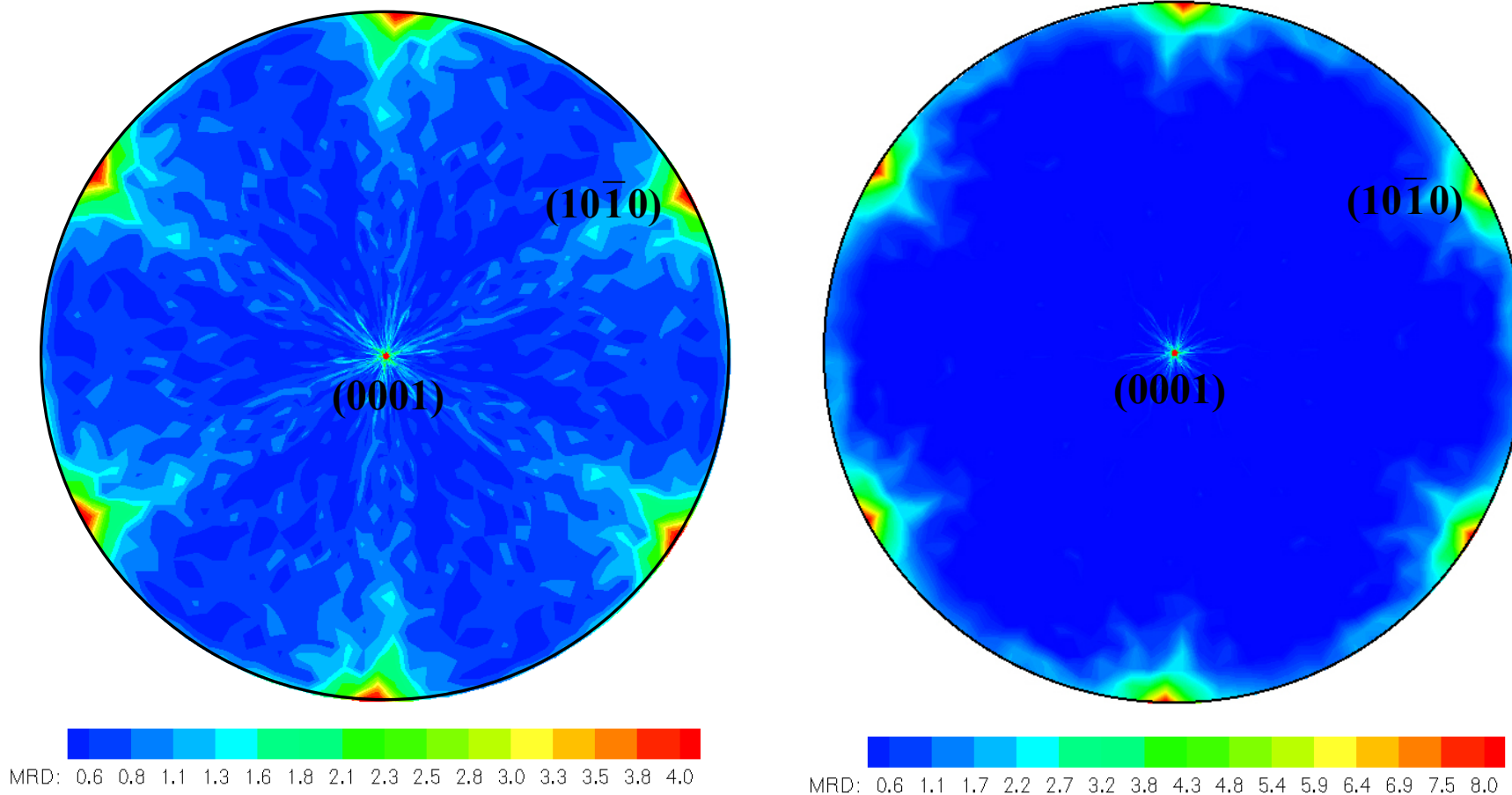
High MRD values occur at the same positions of 50 and 200 WC grain tracings
→ Only 200 grains are needed to determine habit planes because of the small number of facets

There are two habit planes, basal plane (0001) and prism plane $(10\bar{1}0)$

[Changsoo Kim, 2004]

Five parameter grain boundary character distribution (GBCD)
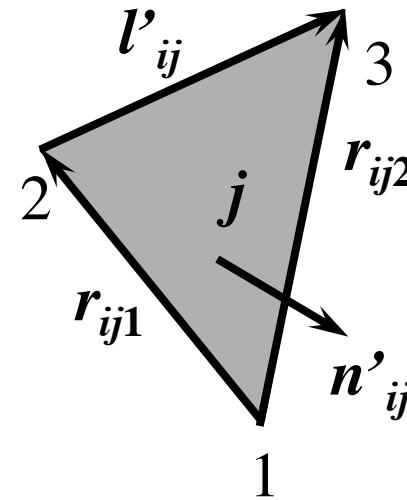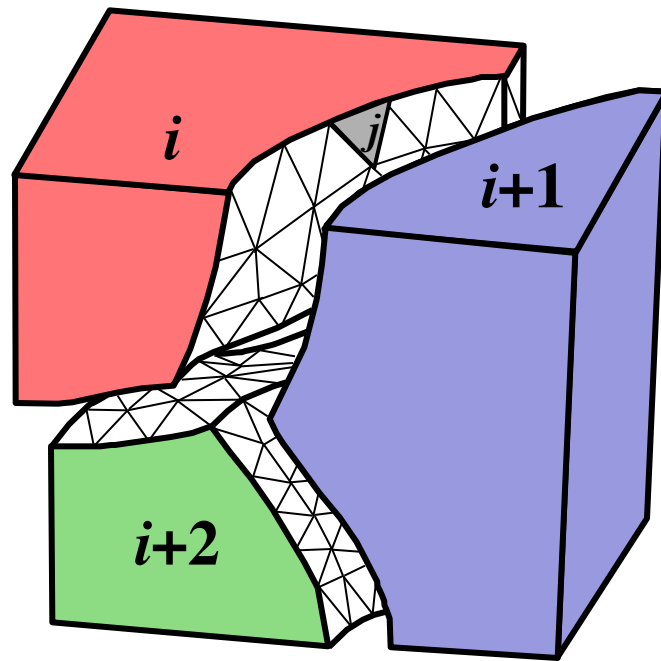
Three parameters for the misorientation: $\Delta g_{i,i+1}$

Two parameters for the orientation: $\mathbf{n}_{ij}$

Grain boundary character distribution: $\lambda(\Delta g, \mathbf{n})$, a normalized area measured in MRD

Direct Measurement of the Five Parameters
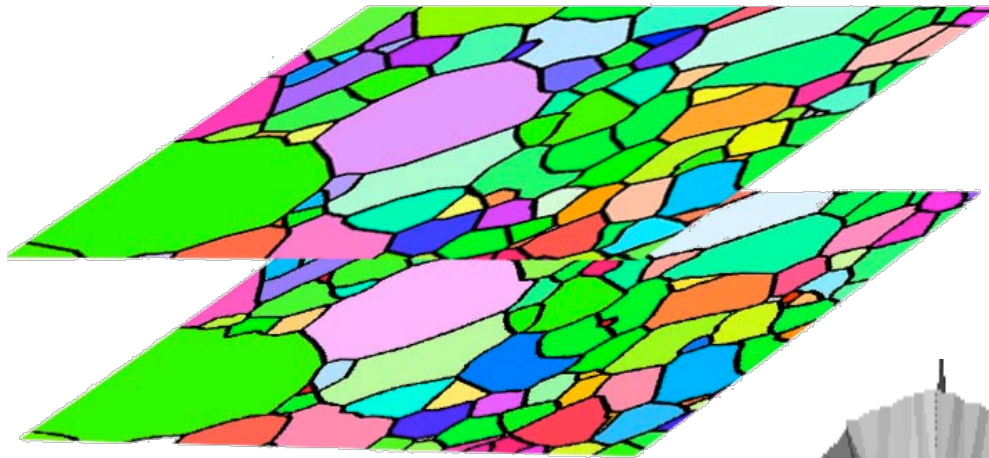
Record high resolution EBSP maps on two adjacent layers.

Assume triangular planes connect boundary segments on the two layers.
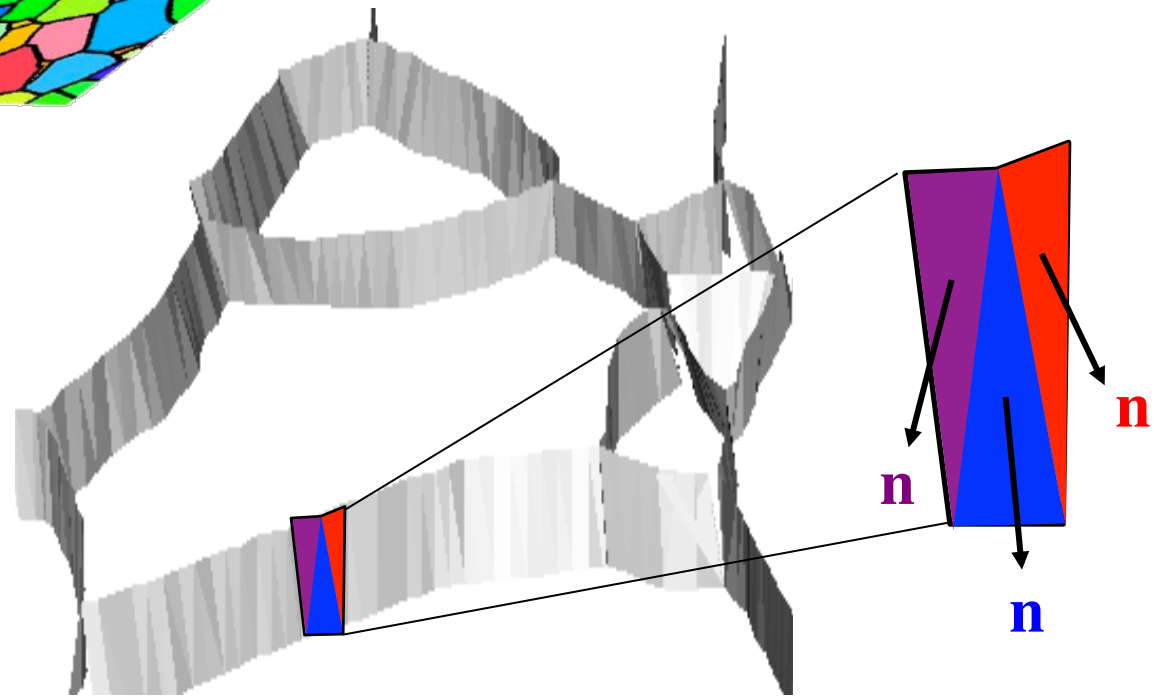
Δg and **n** can be specified for each triangular segment

n

n

n

Saylor, Morawiec, Rohrer, Acta Mater. 51 (2003) 3663

Stereology for Measuring Δg and n
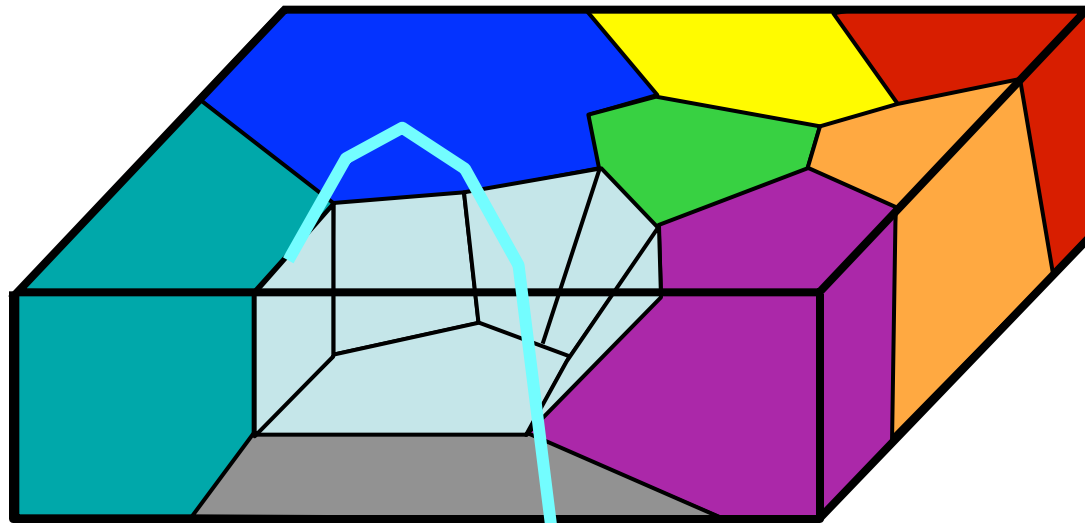
The probability that the correct plane is in the zone is 1.

The probability that all planes are sampled is < 1.

Poles of possible planes

The grain boundary surface trace is the zone axis of the possible boundary planes.
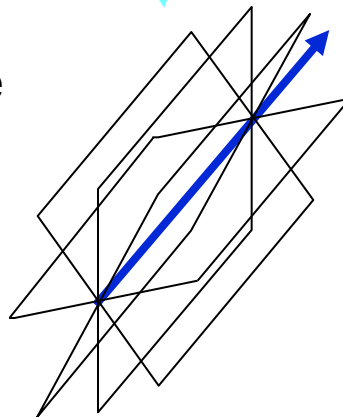
transform to the misorientation reference frame

Δg

Trace pole
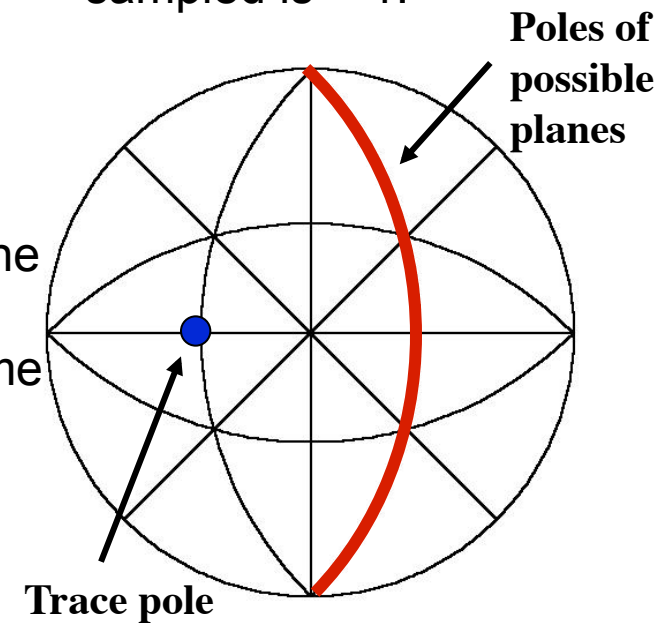
NB each trace contributes two poles, zones, one for each side of the boundary

D.M. Saylor, B.L. Adams, and G.S. Rohrer, "Measuring the Five Parameter Grain Boundary Distribution From Observations of Planar Sections," *Metallurgical and Materials Transactions*, **35A** (2004) 1981-1989.

Illustration of Boundary Stereology

Grain boundary traces in sample reference frame
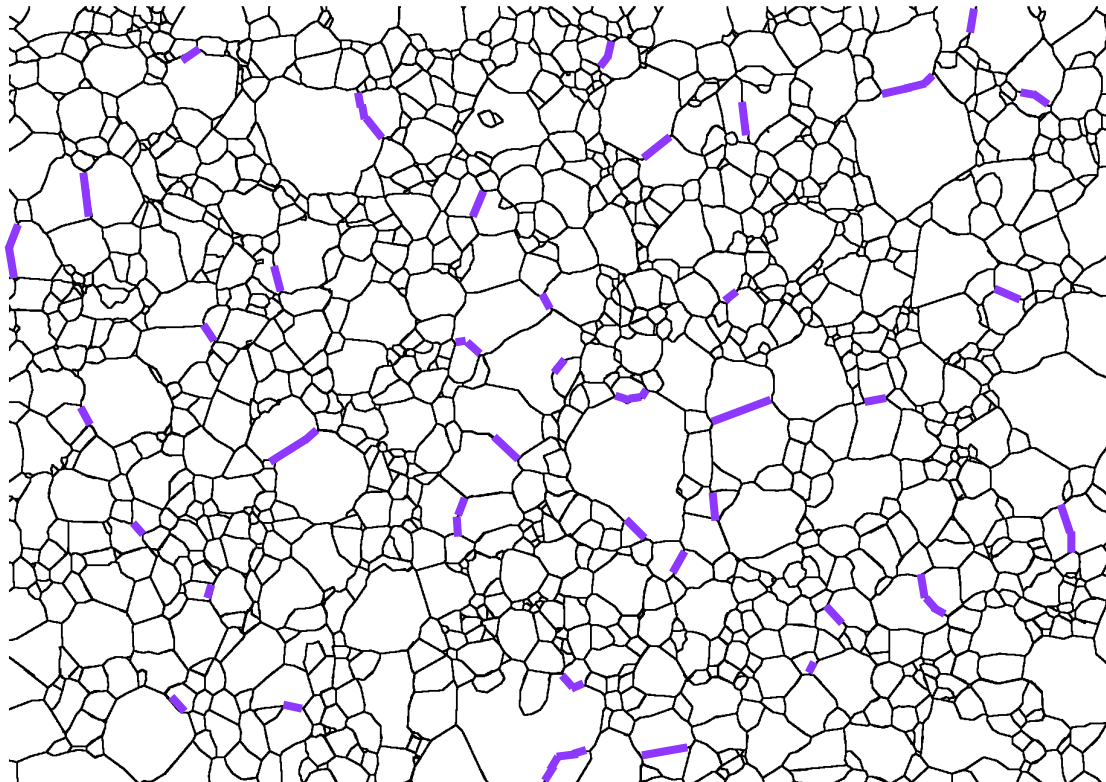
All planes in the zone of trace, in the misorientation frame (at a fixed Δg)
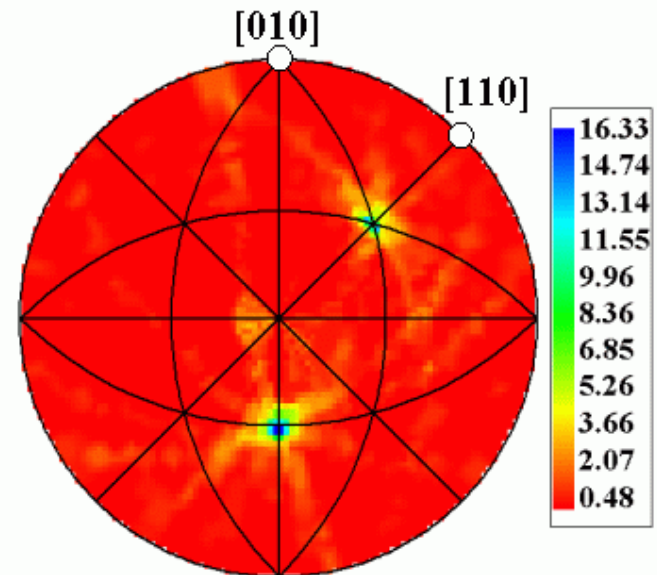
N = 100 and ... subtract

The background of accumulated false signals must then be subtracted.
• **The result is a representation of the true distribution of grain boundary planes at each misorientation.**
• **A continuous distribution requires roughly 2000 traces for each Δg**

Background Subtraction

• Each tangent accumulated contributes intensity both to correct cells (with maxima) and to incorrect cells.

• The closer that two cells are to each other, the higher the probability of "leakage" of intensity. Therefore the calculation of the correction is based on this.

 The correct line length in the ith cell is l_i^c and the observed line length is l_i^o. The discretization is specified by D cells over the angular range of the accumulator (stereogram).

$$l_i^c = \frac{l_i^o - \left(\frac{D-2}{D}\right)\left(\frac{D-1}{D}\right)\langle l^o \rangle}{1 + \left(\frac{2}{D}\right)(D-1)}$$

Background Subtraction: detail

Recall the basic approach for the accumulator diagram:
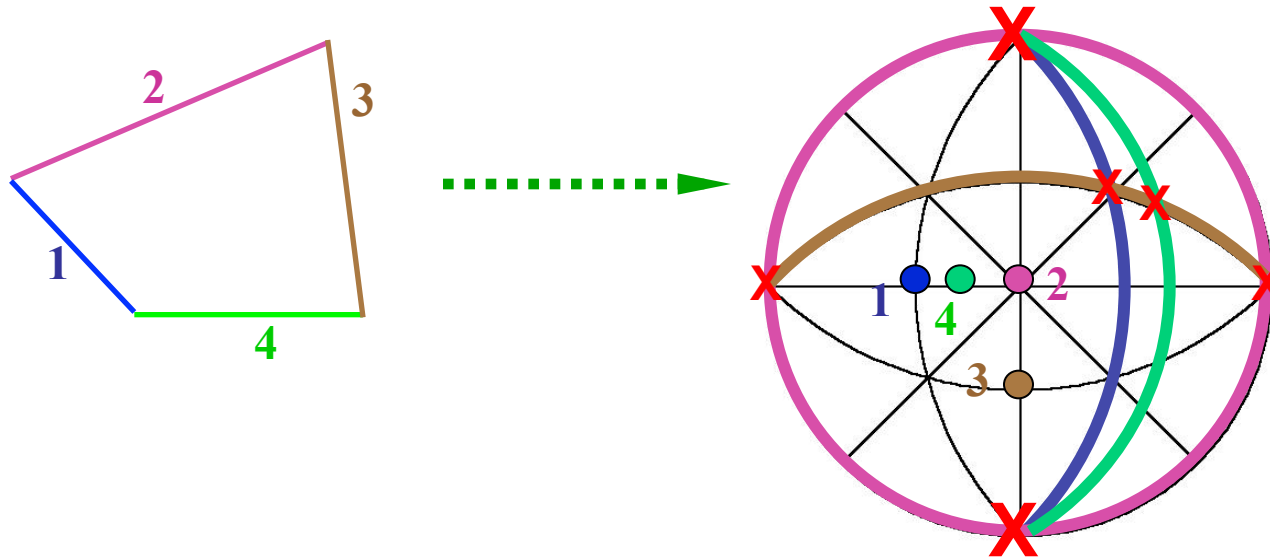
Take the "correct" location of intensity at 111; the density of arcs decreases steadily as one moves away from this location. This is the basis for the non-uniform background correction.

Background Subtraction: detail

The basis for the correction given by Saylor et al. is simplified to two parts.
1. A correction is applied for the background in all cells.
2. A second correction is applied for the nearest neighbor cells to each cell.

In more detail:
1. The first correction uses the average of the intensities in all the cells except the one of interest, and the set of nearest neighbor (NN) cells.
2. The second correction uses the average of the intensities in just the NN cells, because these levels are higher than those of the far cells.

Despite the rather approximate nature of this correction, it appears to function quite well.

Background Subtraction: detail

The correction given by Saylor *et al*. is based on fractions of each line that do not belong to the point of interest. Out of D cells along each line (zone of a trace) *D-1* out of D cells are background. The first order correction is therefore to subtract *(D-1)/D* multiplied by the average intensity, from the intensity in the cell of interest (the ith cell).

This is then further corrected for the higher background in the *NN* cells by removing a fraction *Z (=2/D)* of this amount and replacing it with a larger quantity, *Z(D-1)* multiplied by the intensity in the cell of interest (l_i^c).

$$l_i^c \approx l_i^o + (Z - 1)\frac{(D-1)}{D}\langle l^o \rangle - Z(D-1)l_i^c$$

Texture effects, limitations

- If the (orientation) texture of the material is too strong, the method as described will not work.

- Texture effects can be mitigated by taking sections with different normals, e.g. slices perpendicular to the RD, TD, ND.

- No theory is available for how to quantify this issue (e.g. how many sections are required?).

Examples of 2-Parameter GBCD

- *Important limitation of the stereological approach: it assumes that the (orientation) texture of the material is negligible.*

- The next several slides show examples of 2-parameter and 5-parameter distributions from various materials.

- The 2-parameter distributions are equivalent to posing the question "how does the boundary population vary with plane/normal, regardless of misorientation?"

- Intensities are given in terms of multiples of a random (uniform) intensity (MRD/MUD).

- Grain boundary populations are computed for only the boundary normal (and the misorientation is "averaged out"). These can be compared with surface energies.

Examples of Two Parameter Distributions

**Grain Boundary
Population (Δg averaged)**

**Measured Surface
Energies**

MgO
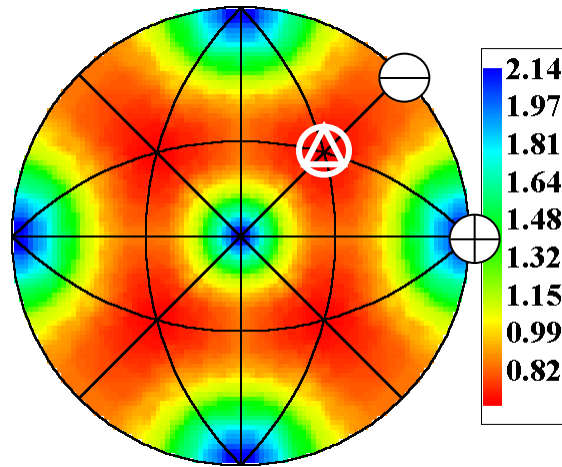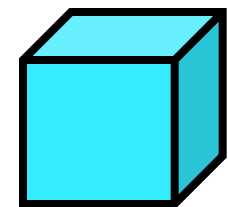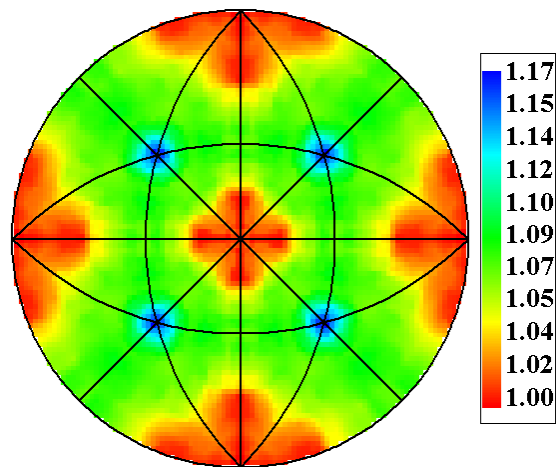
Saylor & Rohrer, Inter. Sci. 9 (2001) 35.

SrTiO$_3$
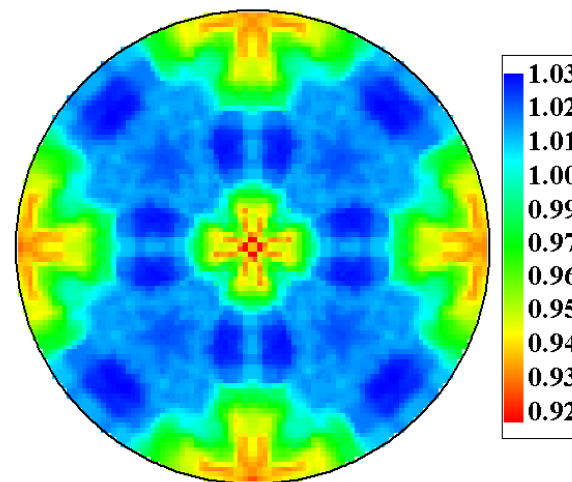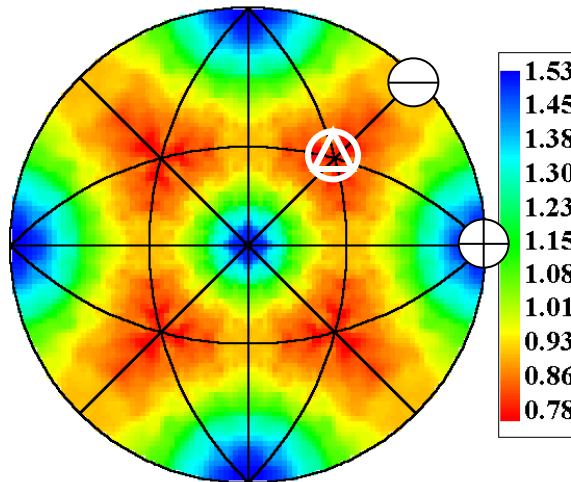
Sano et al., J. Amer. Ceram. Soc., 86 (2003) 1933.

Examples of Two Parameter Distributions

**Grain Boundary
Population (Δg averaged)**

**Surface Energies/
habit planes**

$MgAl_2O_4$

TiO_2
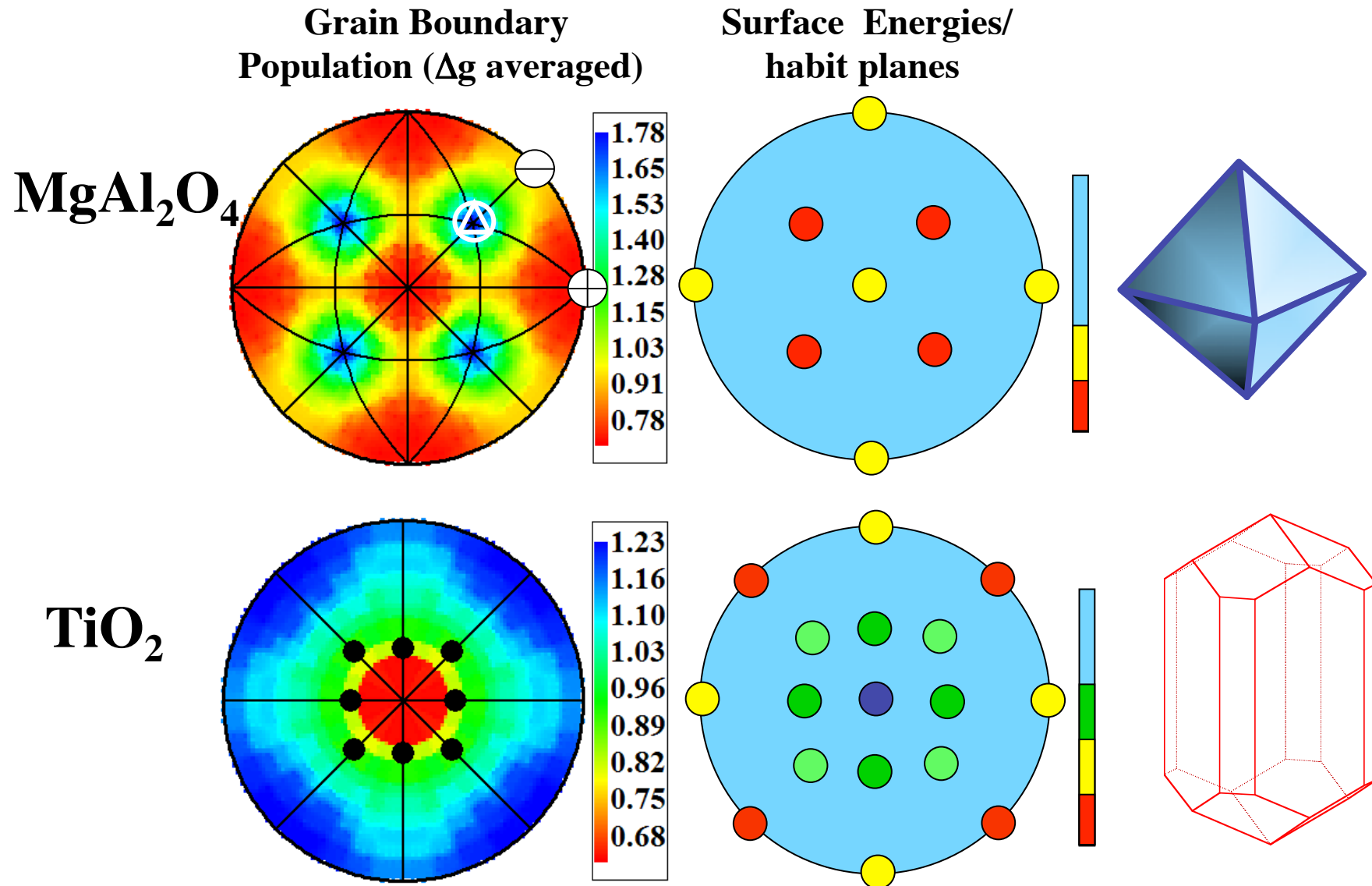
Ramamoorthy et al., *Phys. Rev. B* **49** (1994)**16721.**

Examples of Two Parameter Distributions

**Grain Boundary
Population (Δg averaged)**

**Surface Energies/
habits**

Al$_2$O$_3$

2.20
1.99
1.77
1.56
1.34
1.13
0.92
0.71
0.49
0.28
0.07

1.00<γ

1.00

0.95
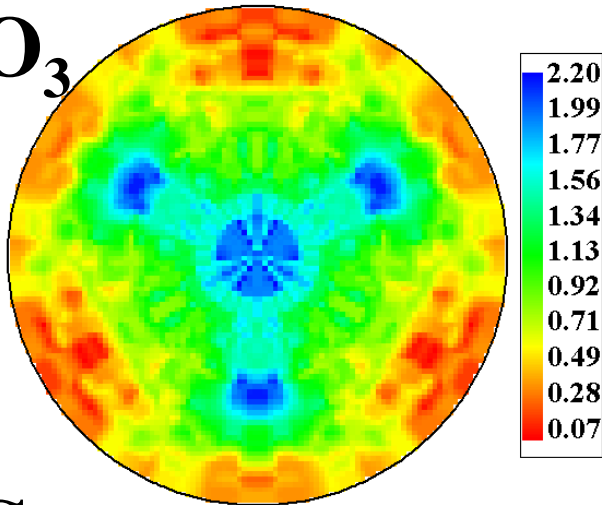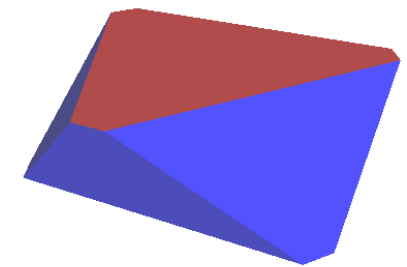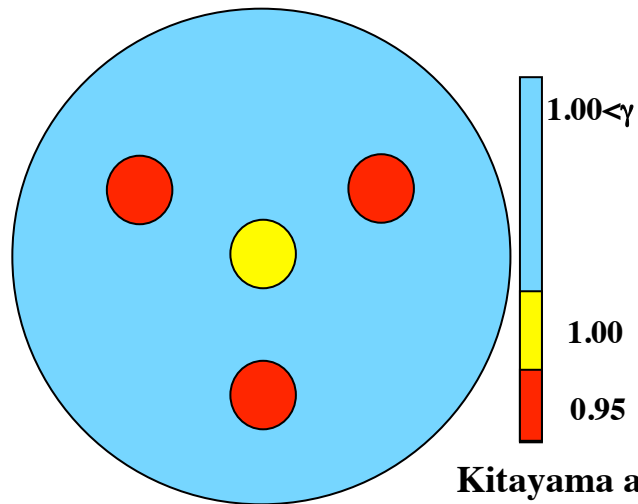
**Kitayama and Glaeser,
JACerS, 85 (2002) 611.**

WC
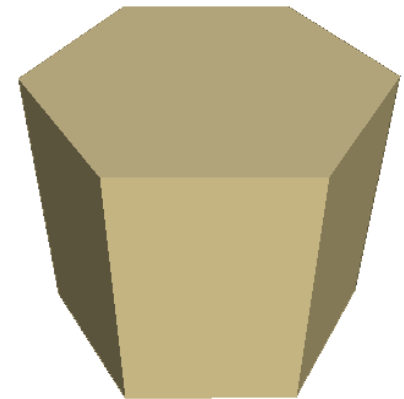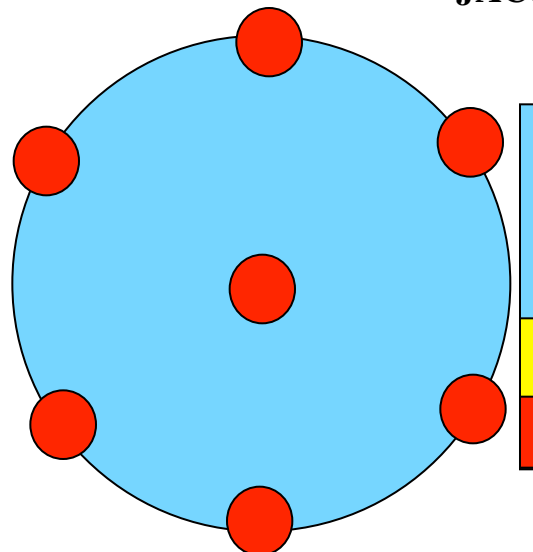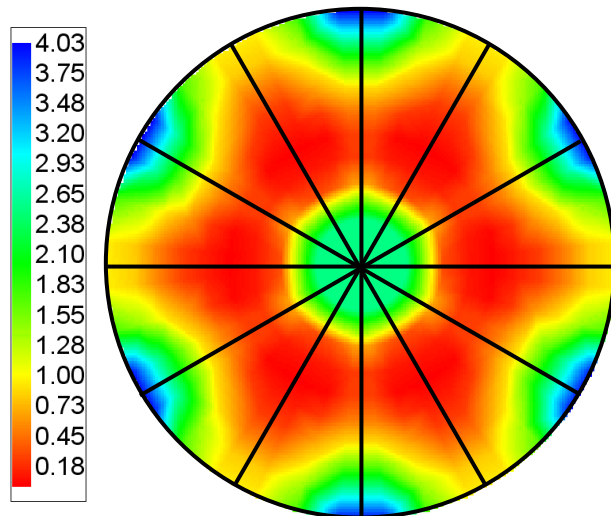
4.03
3.75
3.48
3.20
2.93
2.65
2.38
2.10
1.83
1.55
1.28
1.00
0.73
0.45
0.18

Examples of Two Parameter Distributions

**Grain Boundary
Population (Δg averaged)**

**Measured Surface
Energies**

Al
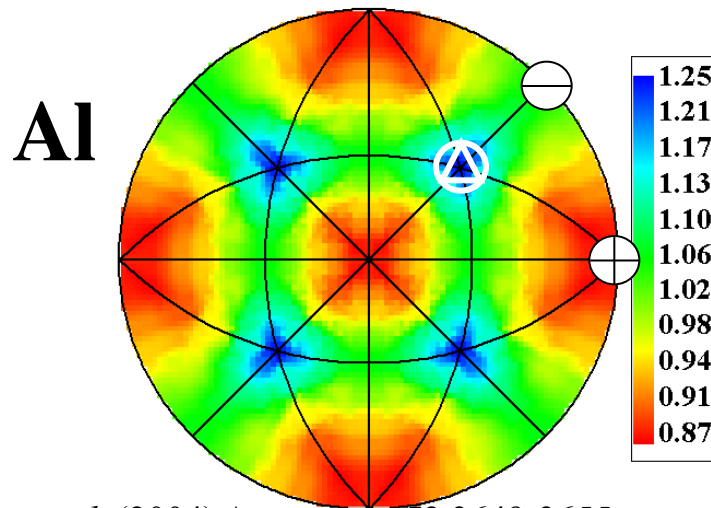
Saylor *et al*. (2004) Acta mater. **52** 3649-3655
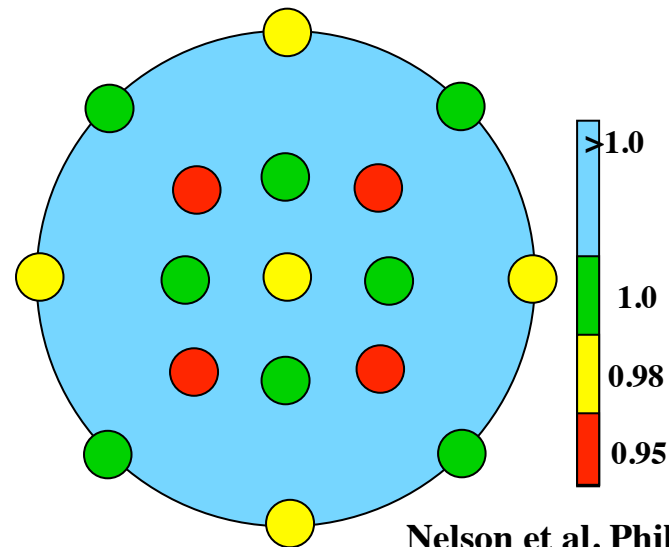
Nelson et al. Phil. Mag. 11 (1965) 91.
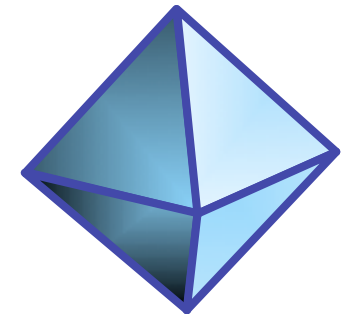
Fe-Si
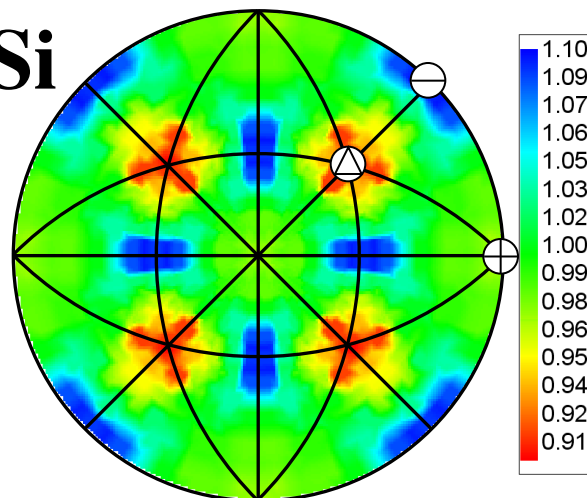
Bennett *et al*. (2004) Recrystallization and Grain Growth, **467-470**: 727-732
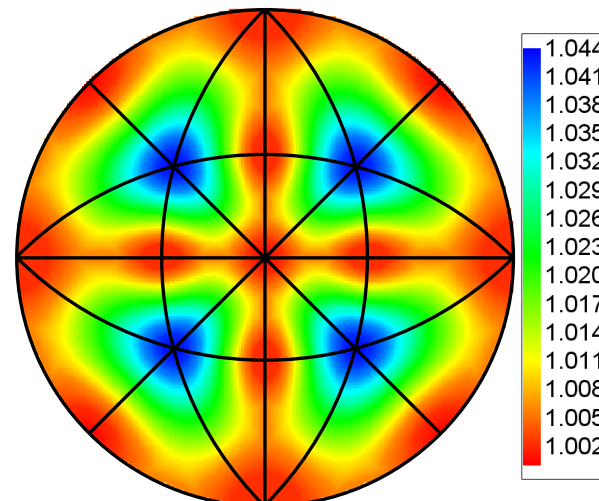
Gale et al. Phil. Mag. 25 (1972) 947.
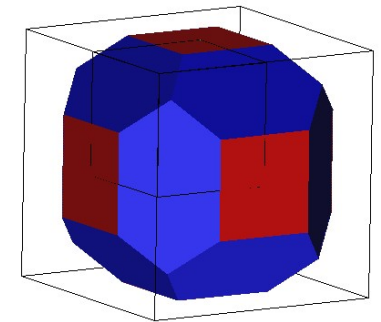
Examples of 5-parameter GBCDs

- Next, we consider how the population varies when the misorientation is taken into account

- Each stereogram corresponds to an individual misorientation: as a consequence, the crystal symmetry is (in general) absent because the misorientation axis is located in a particular asymmetric zone in the stereogram.

- It is interesting to compare the populations to those that would be predicted by the CSL approach.

- Note that the *pure twist boundary* is represented by normals parallel to (coincident with) the misorientation axis. *Pure tilt boundaries* lie on the zone of the misorientation axis.

- The misorientation axis is always placed in the 100-110-111 triangle.
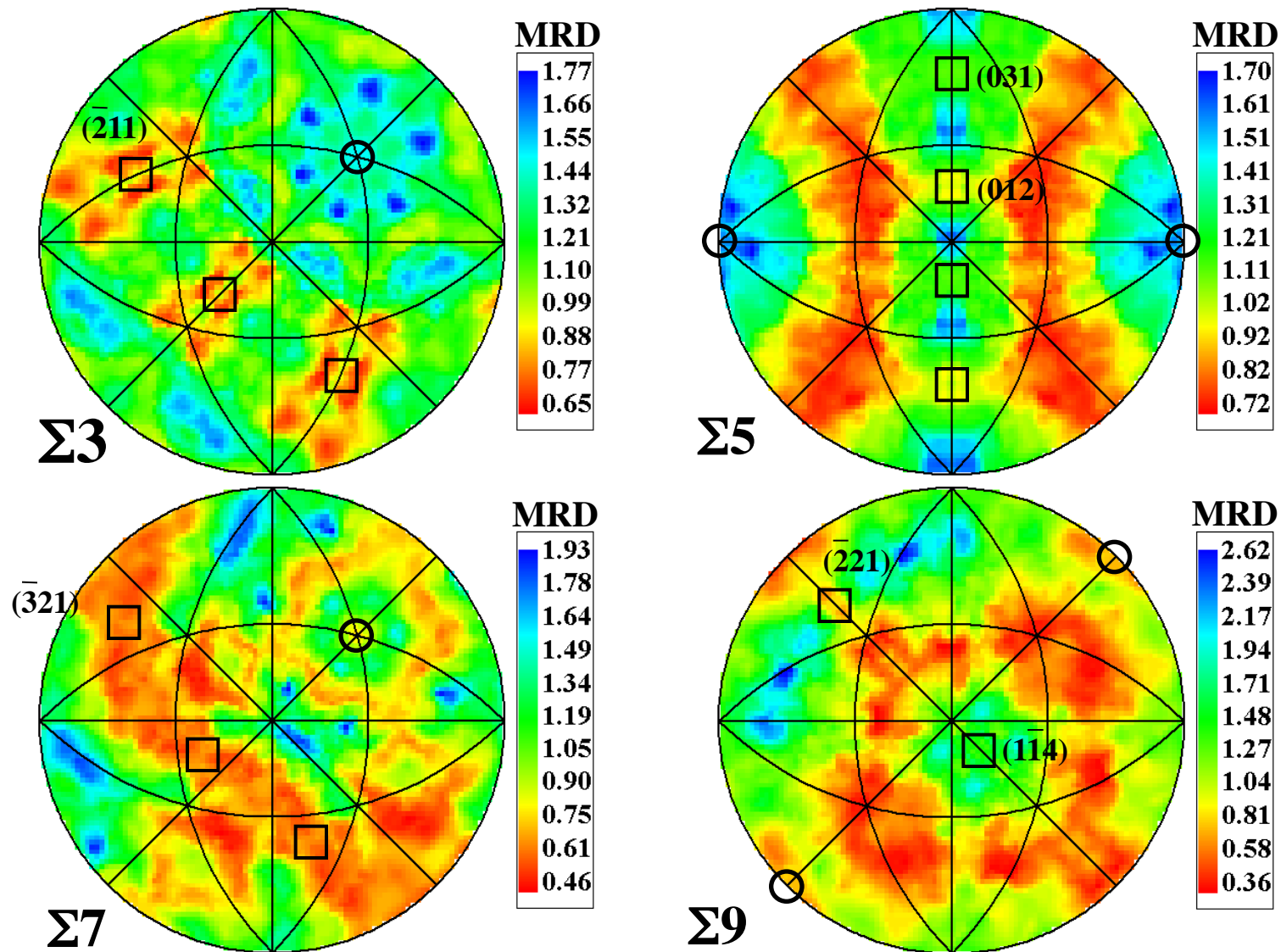
Grain Boundary Distribution in Al: [111] axes

Misorientation axis always in this SST

$\lambda(\mathbf{n})$

$\lambda(\Delta \mathbf{g}, \mathbf{n})$

$\lambda(\mathbf{n}|40°/[110])$

MRD

(a)

(b) 40°≈Σ9
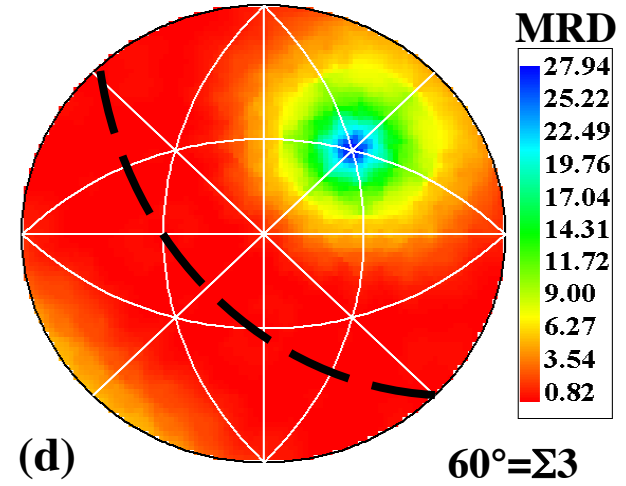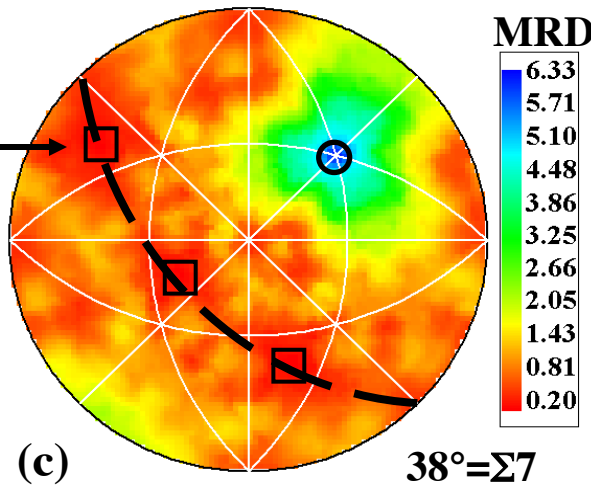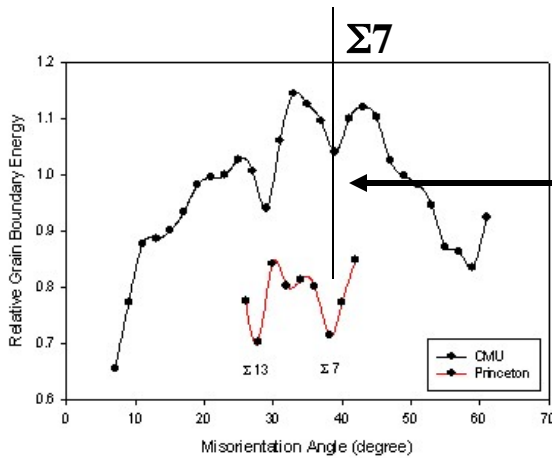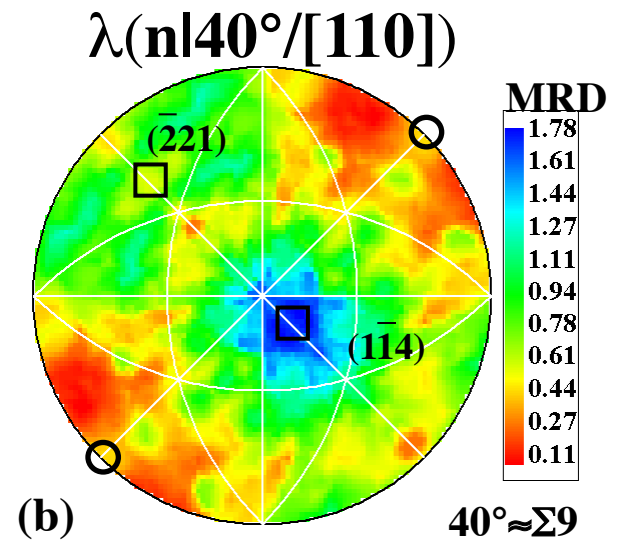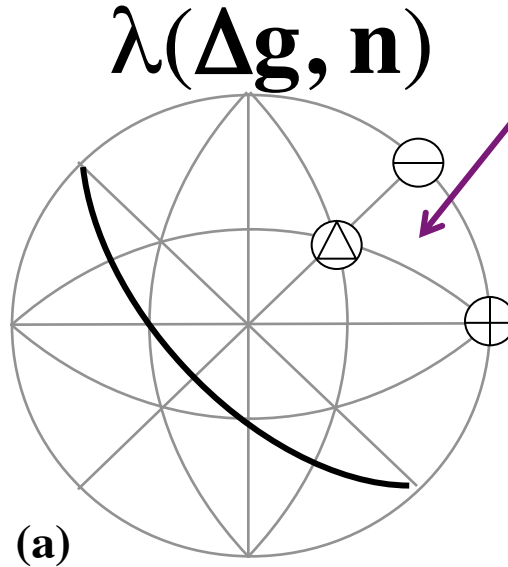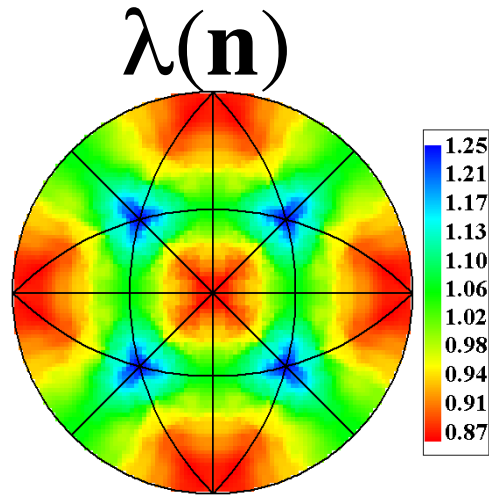
<111> tilt boundaries analyzed in an Al thin film, annealed at 400°C.

$\lambda(\mathbf{n}|38°/[111])$

(c) 38°=Σ7

$\lambda(\mathbf{n}|60°/[111])$

(d) 60°=Σ3

(111) Twist boundaries are the dominant feature in $\lambda(\Delta \mathbf{g}, \mathbf{n})$

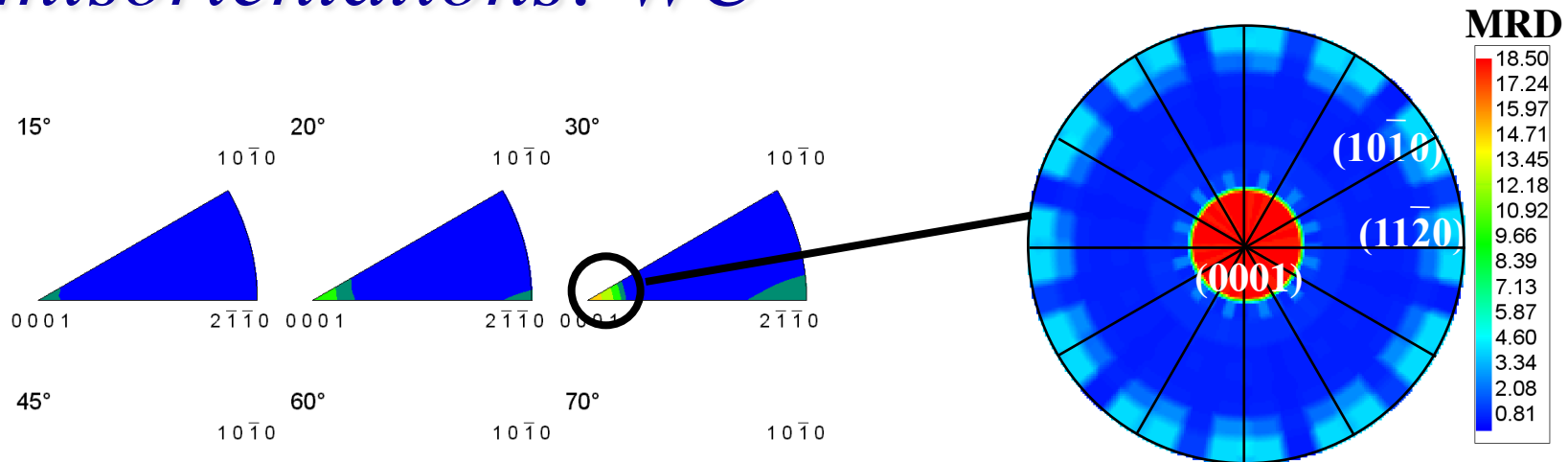# $\lambda(n)$ for low Σ CSL misorientations: $SrTiO_3$

Except for the coherent twin, high lattice coincidence and high planar coincidence do not explain the variations in the grain boundary population.

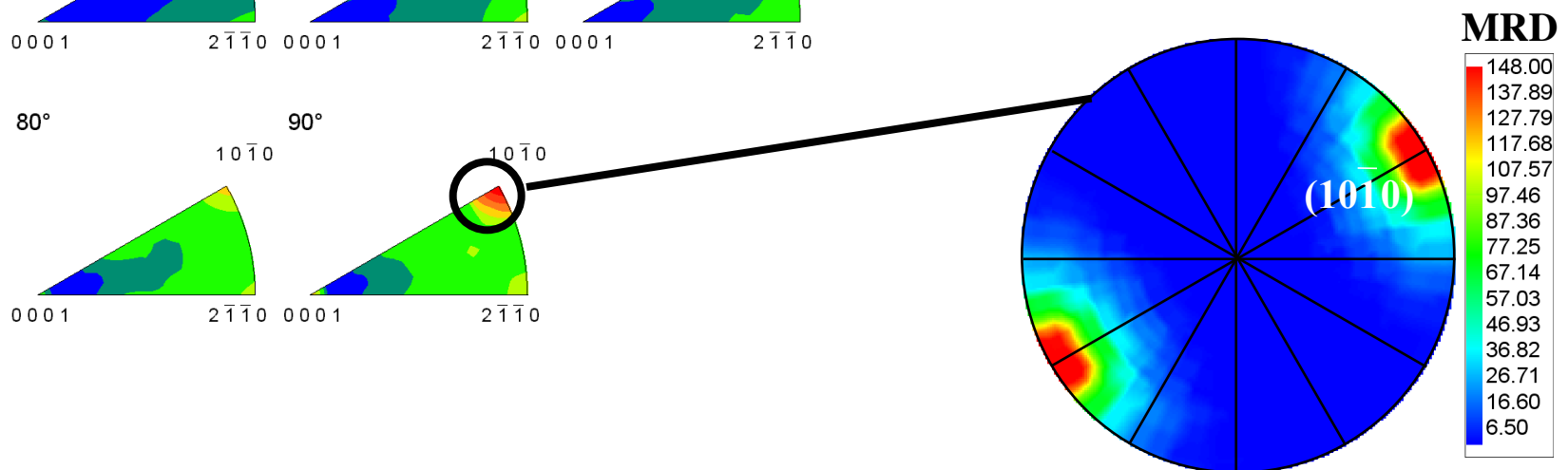# *Distribution of planes at a single misorientation*

λ(n|66°[100])

Twin in TiO_2
66° around [100]
or, 180° around <101>

33.00
30.75
28.49
26.24
23.99
21.73
19.48
17.22
14.97
12.72
10.46
8.21
5.96
3.70
1.45

□ [100]

(011)
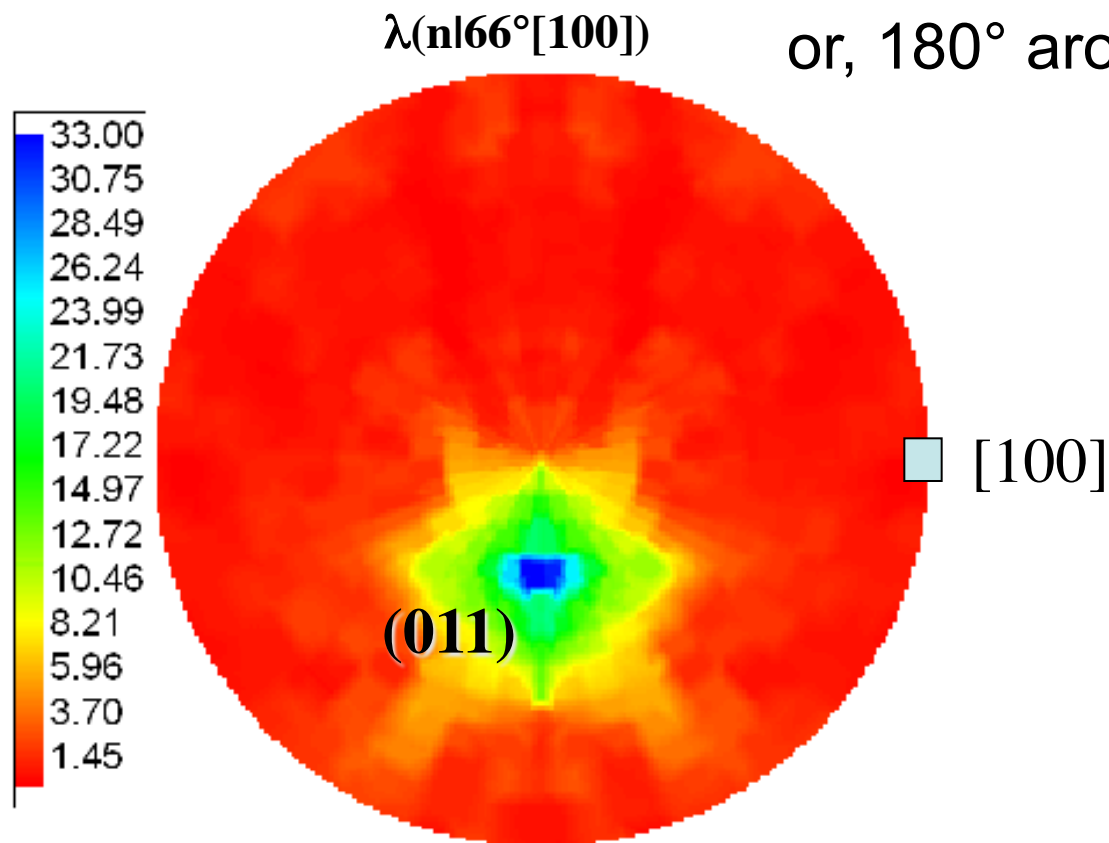
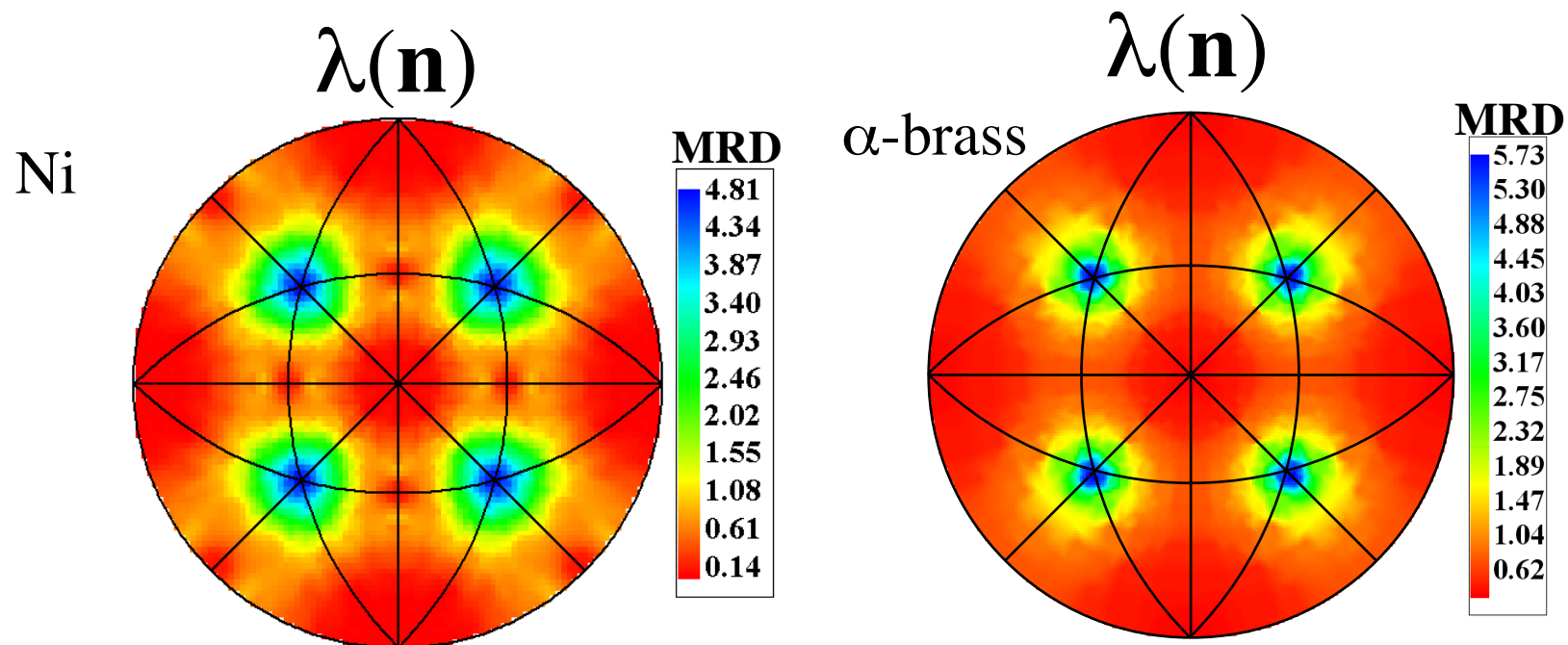# Distribution of planes at a single misorientations: WC

Plane orientations for grain boundaries
with a 30° misorientation about [0001]

Plane orientations for grain boundaries
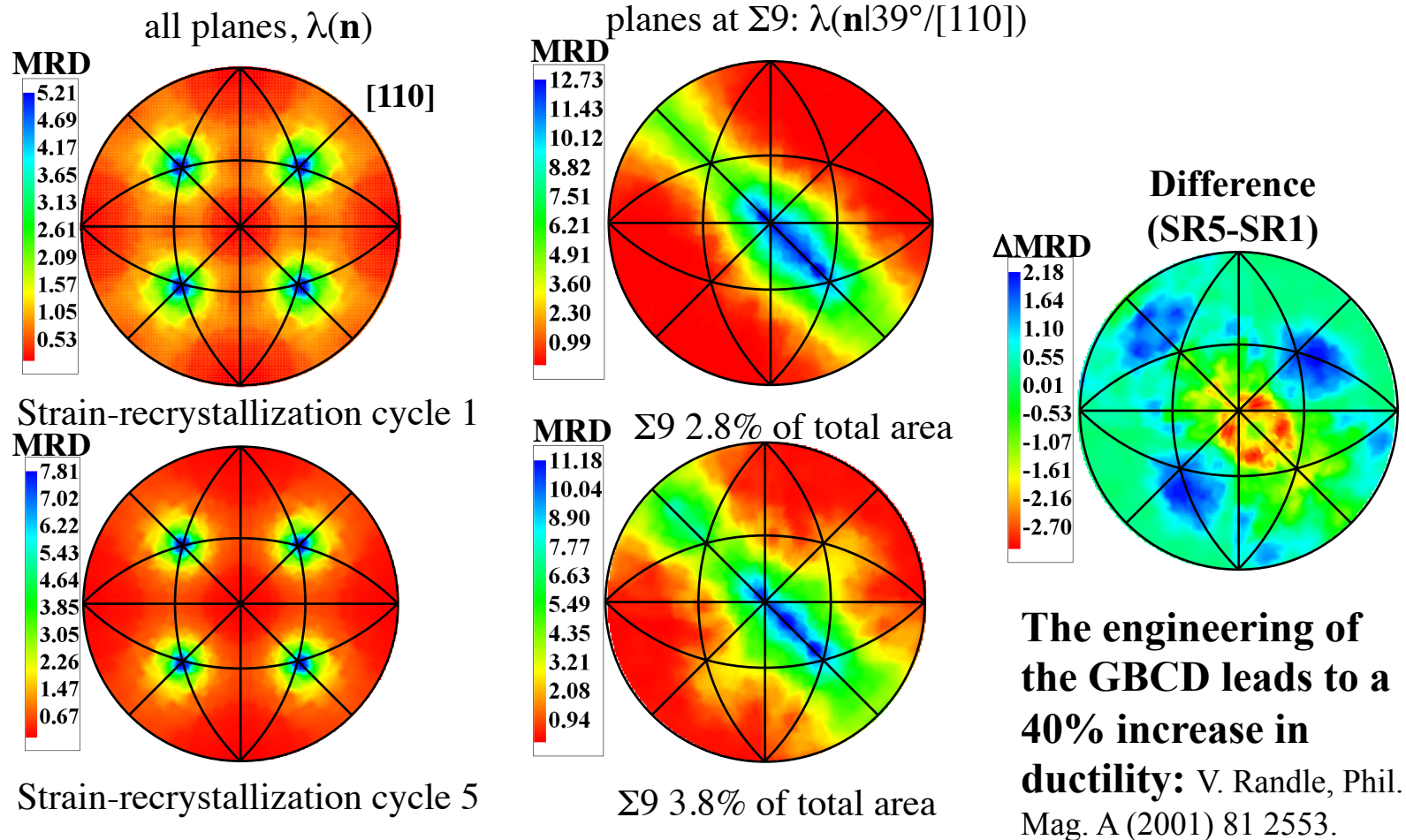with a 90° misorientation about [10$\bar{1}$0]

Cubic close packed metals with low stacking fault energies

Preference for the (111) plane is stronger than in Al, but this is mainly a consequence of the high frequency of annealing twins in low to medium stacking-fault energy fcc metals.

# *Influence of GBCD on Properties: Experiment*

Grain Boundary Engineered α-Brass

all planes, λ(**n**)

MRD
5.21
4.69
4.17
3.65
3.13
2.61
2.09
1.57
1.05
0.53

[110]

planes at Σ9: λ(**n**|39°/[110])

MRD
12.73
11.43
10.12
8.82
7.51
6.21
4.91
3.60
2.30
0.99

Strain-recrystallization cycle 1

MRD
7.81
7.02
6.22
5.43
4.64
3.85
3.05
2.26
1.47
0.67

MRD   Σ9 2.8% of total area
11.18
10.04
8.90
7.77
6.63
5.49
4.35
3.21
2.08
0.94

Strain-recrystallization cycle 5

Σ9 3.8% of total area

**Difference
(SR5-SR1)**

ΔMRD
2.18
1.64
1.10
0.55
0.01
-0.53
-1.07
-1.61
-2.16
-2.70

**The engineering of
the GBCD leads to a
40% increase in
ductility:** V. Randle, Phil.
Mag. A (2001) 81 2553.

The increase in ductility can be linked to increased dislocation
transmission at grain boundaries.

Effect of GB Engineering on GBCD

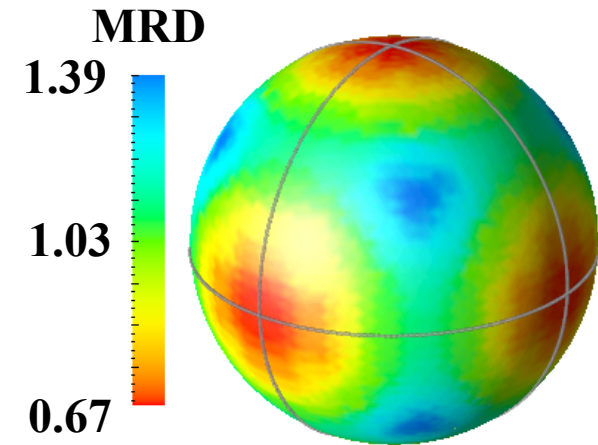**λ(n), averaged over all misorientations (Δg)**

α-brass

Can processes that are not permitted to reach steady state be predicted from steady state behavior (grain boundary engineering)?
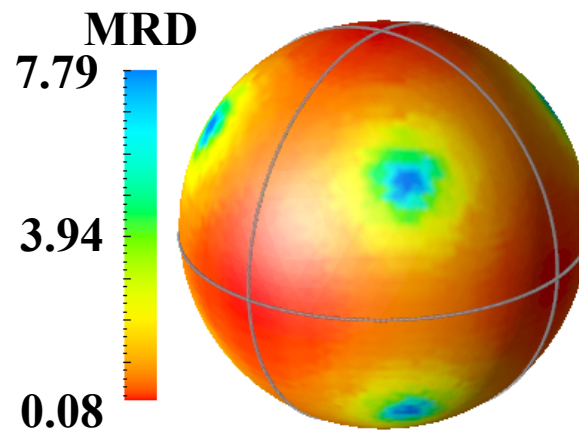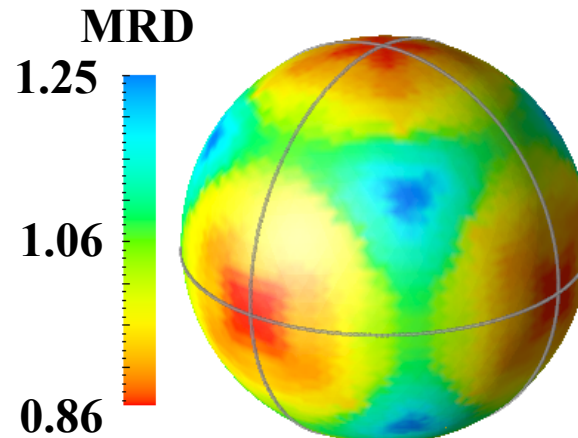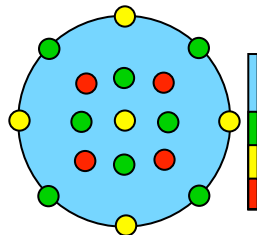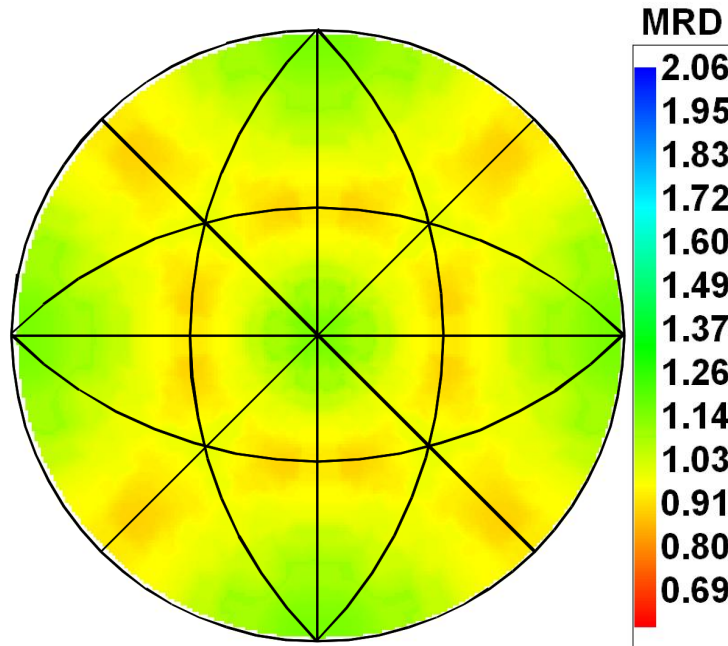
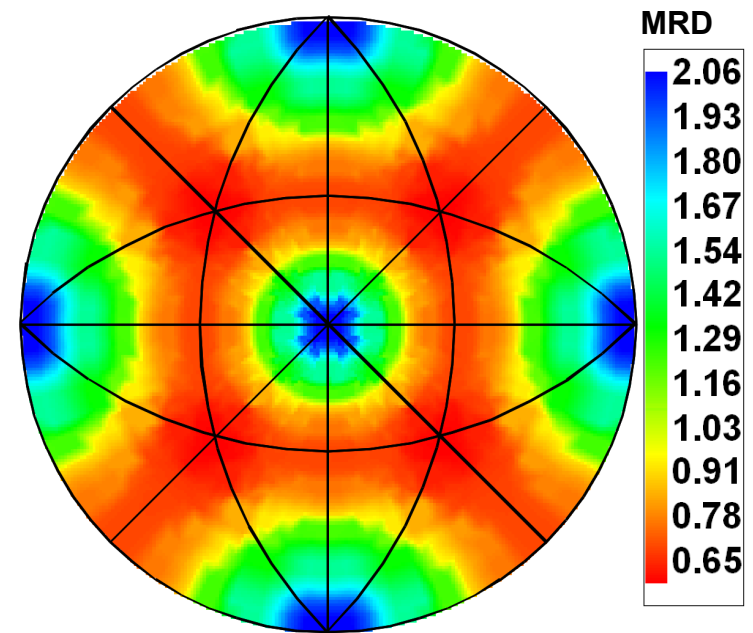

all boundaries

twins removed

Al

With the exception of the twins, GBE brass is similar to Al

Experiment: compare the GBCD and GBED for pure (undoped) and doped materials
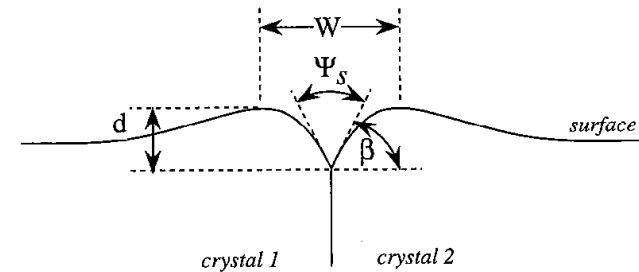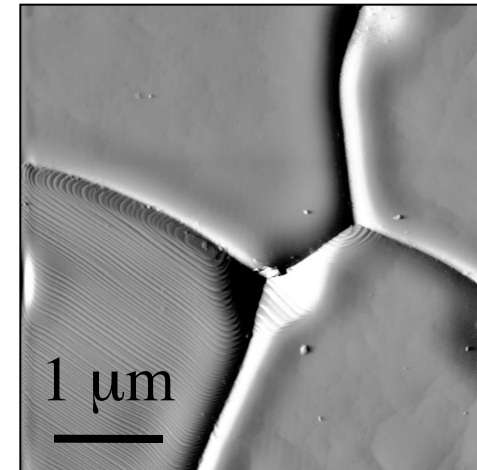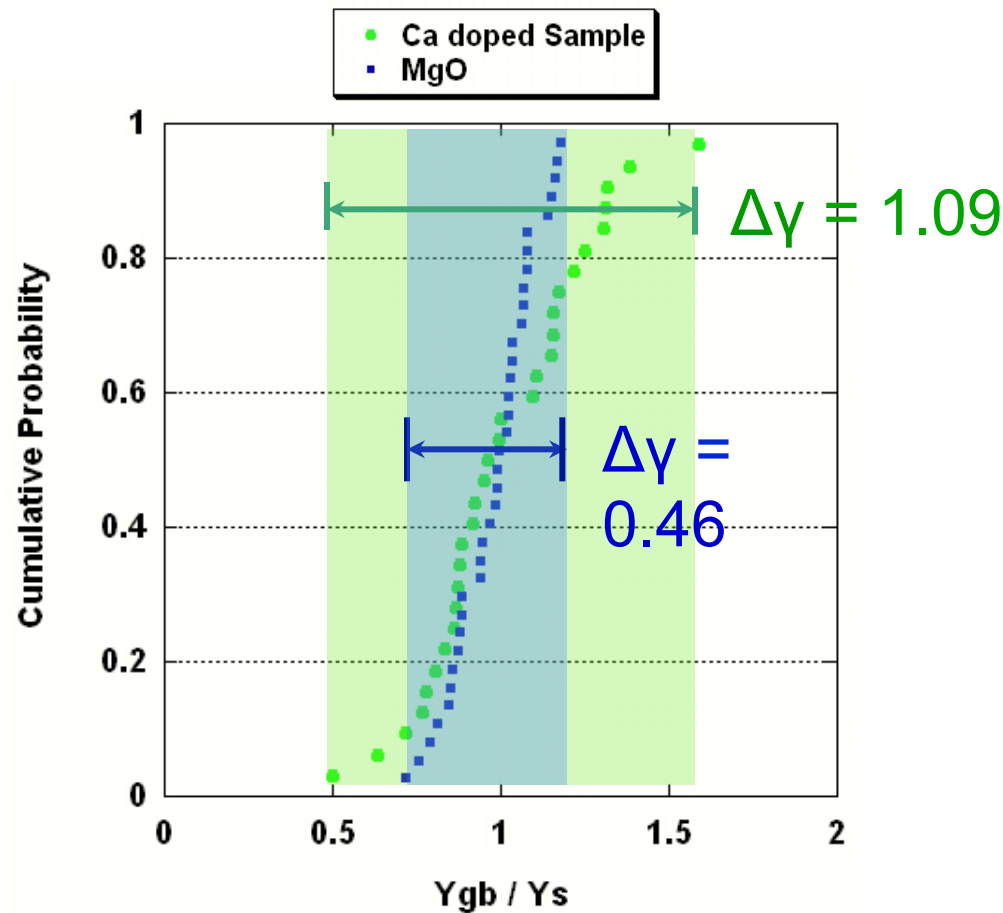

Undoped MgO, grain size: 24μm

Ca-doped MgO, grain size: 24μm

Larger GB frequency range of Ca-doped MgO suggests a larger GB energy anisotropy than for undoped MgO

Grain Boundary Energy Distribution is Affected by Composition

Legend:
- Ca doped Sample
- MgO

$\Delta\gamma = 1.09$

$\Delta\gamma = 0.46$

1 μm

$$\frac{\gamma_{gb}}{\gamma_s} = 2 \cos \frac{\psi_s}{2}$$

Ca solute increases the range of the γ_{gb}/γ_s ratio.
The variation of the relative energy in undoped MgO is lower (narrower distribution) than in the case of doped material.

76

Bi impurities in Ni have the opposite effect

Pure Ni, grain size: 20μm

Bi-doped Ni, grain size: 21μm
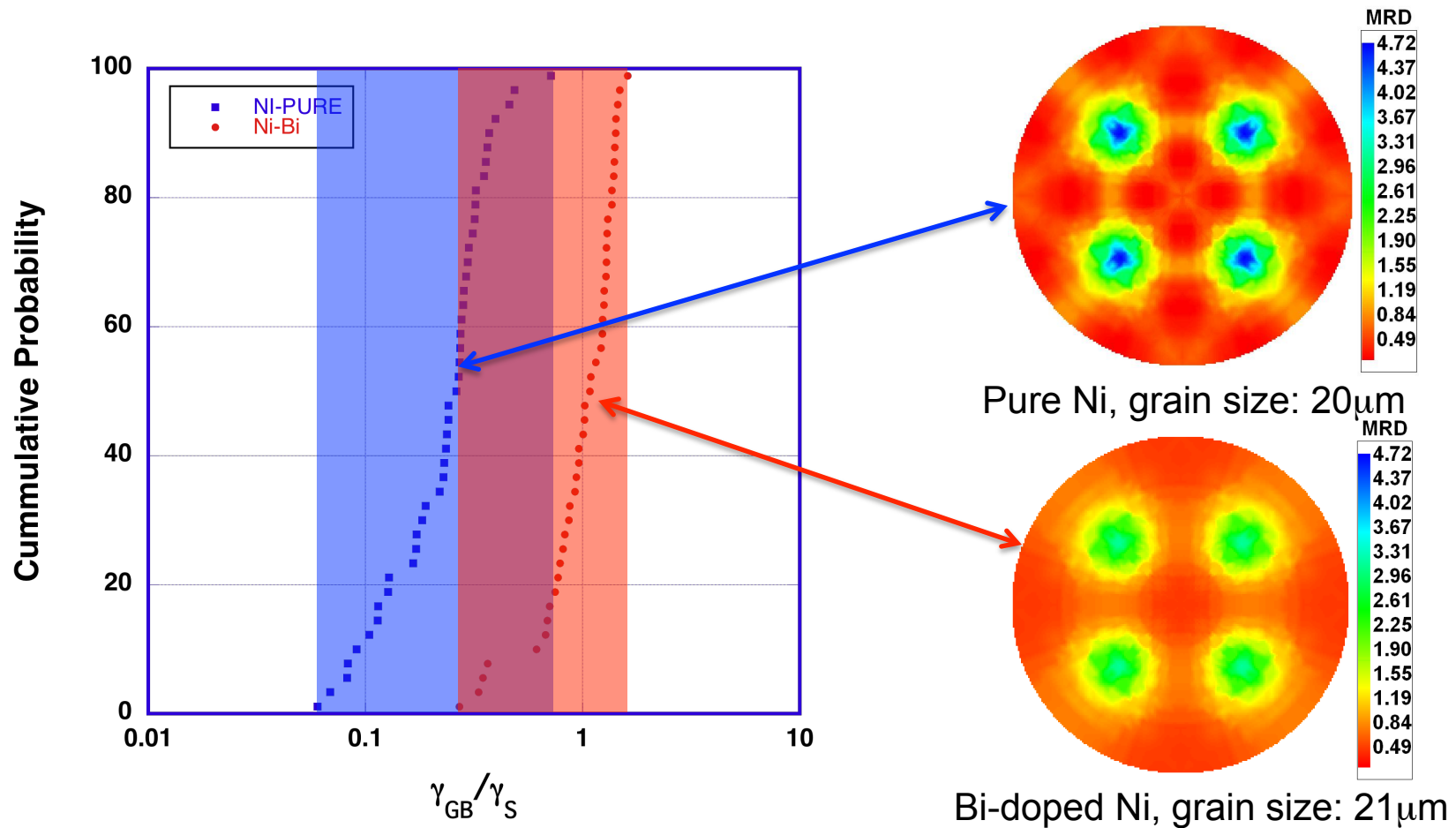
Range of γ_{GB}/γ_S (on log scale) is smaller for Bi-doped Ni than for pure Ni, indicating smaller anisotropy of γ_{GB}/γ_S. This correlates with the plane distribution

Conclusions

• Statistical stereology can be used to reconstruct a most probable distribution of boundary normals, based on their traces on a single section plane.

• Thus, the full 5-parameter Grain Boundary Character Distribution can be obtained stereologically from plane sections, provided that the texture is weak.

• The tendency for grain boundaries to terminate on planes of low index and low energy is widespread in materials with a variety of symmetries and cohesive forces.

• The observations reduce the apparent complexity of interfacial networks and suggest that the mechanisms of solid state grain growth may be analogous to conventional crystal growth.

Questions

- What is an accumulator diagram?

- Why do we transform grain boundary traces from the sample frame to the crystal frame?

- What is stereology?

- Which quantities can be measured directly from cross-sections?

- What is the stereological relationship between line length (e.g. of grain boundaries) measured in cross-section to surface area per unit volume?

- How does frequency of grain boundary type relate to surface energy?

Questions - 2

- What is the significance, if any of the CSL concept in terms of grain boundary populations?

- Which CSL types are actually observed in large numbers (and in which materials)?

- How does grain boundary frequency relate to grain boundary energy?

- What is "Buffon's Needle"?

- How does stereology help us to measure the Grain Boundary Character Distribution?

- What are typical 1-, 3-, 5- and 2-parameter plots of GB character?

Supplemental Slides

- Details about how to construct the zone to an individual pole in a stereogram that represents a (hemi-)spherical space.

- Details about how texture affects the stereological approach to determining GBCD.

Boundary Tangents

- A more detailed approach is as follows.
- Measure the (local) boundary tangent: the normal must lie in its zone.
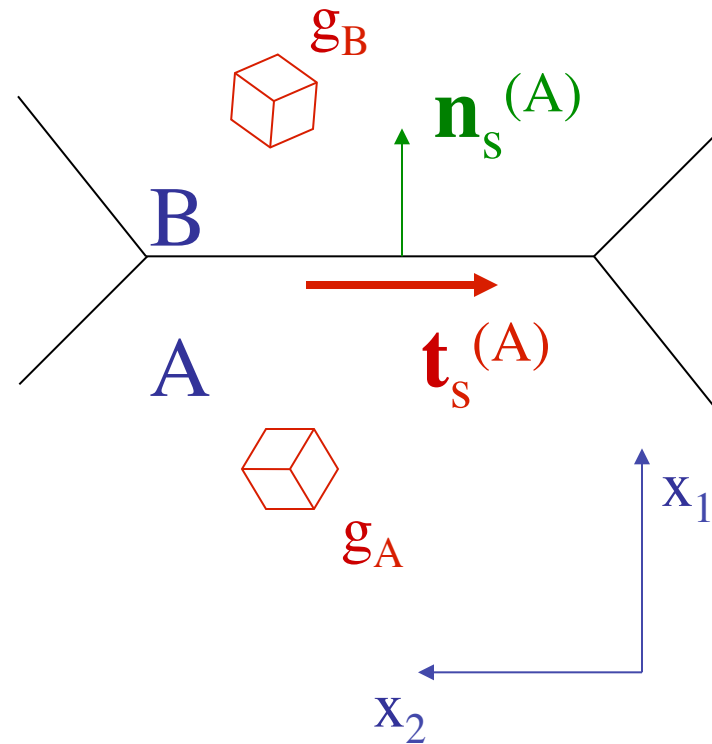
G.B. tangent: disorientation

- Select the pair of symmetry operators that identifies the *disorientation*, i.e. minimum angle *and* the axis in the SST.

$$\Delta g' \xleftrightarrow{=} O^B_{crystalB} \Delta g O^A_{crystalA}$$

$$\hat{\rho}' = \begin{pmatrix} u \\ v \\ w \end{pmatrix} = \begin{bmatrix} [\Delta g'(2,3) - \Delta g'(3,2)]/norm \\ [\Delta g'(1,3) - \Delta g'(3,1)]/norm \\ [\Delta g'(1,2) - \Delta g'(2,1)]/norm \end{bmatrix}$$

$$norm = \sqrt{[\Delta g'(2,3) - \Delta g'(3,2)]^2 + [\Delta g'(1,3) - \Delta g'(3,1)]^2 + [\Delta g'(1,2) - \Delta g'(2,1)]^2}$$

Tangent → Boundary space

- Next we apply the *same symmetry operator* to the tangent so that we can plot it on the same axes as the disorientation axis.

- We transform the zone of the tangent into a great circle.

Boundary planes lie on zone
of the boundary tangent: in this example
the tangent happens to be coincident with
the disorientation axis.

(11̄1̄) Pole

(111) Plane

Disorientation axis
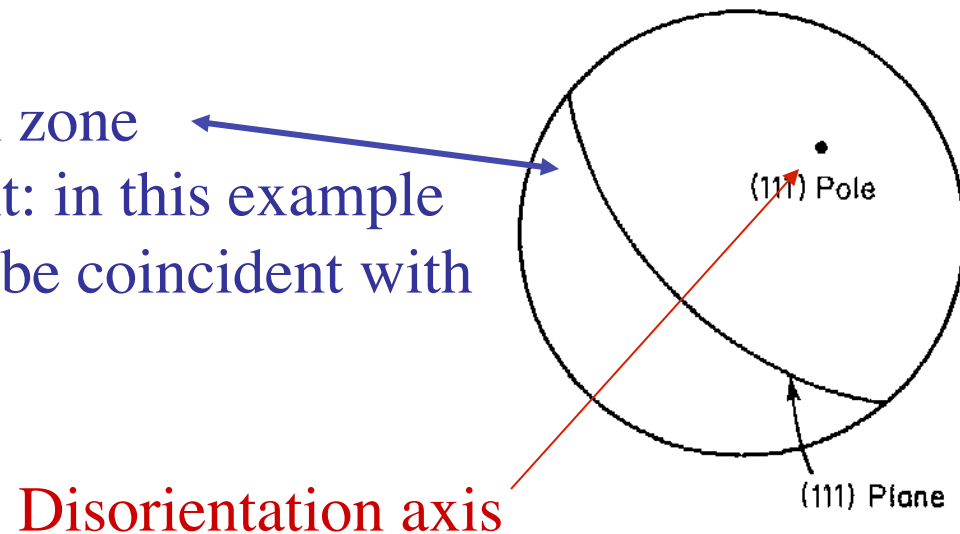
Tangent Zone

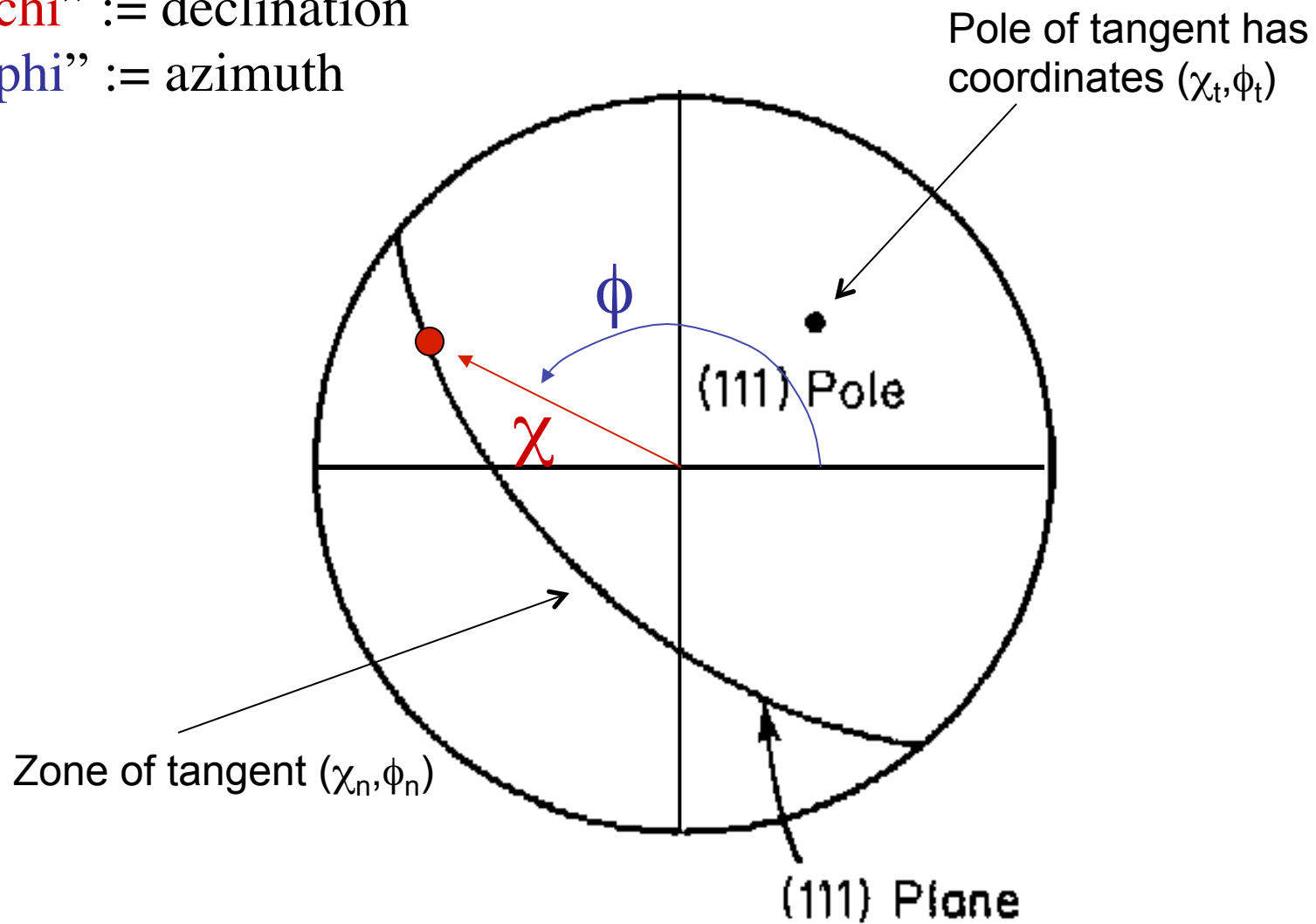- The tangent transforms thus:

$$\mathbf{t}_A = O_A g_A \mathbf{t}_S{}^{(A)}$$

- This puts the tangent into the boundary plane (A) space.

- To be able to plot the great circle that represent its great circle, consider spherical angles for the tangent, $\{\chi_t, \phi_t\}$, and for the zone (on which the normal must lie), $\{\chi_n, \phi_n\}$.

Spherical angles

"chi" := declination
"phi" := azimuth

Pole of tangent has
coordinates (χ_t, ϕ_t)

ϕ

(111) Pole

χ

Zone of tangent (χ_n, ϕ_n)

(111) Plane

Tangent Zone, parameterized

- The scalar product of the (unit) vectors representing the tangent and its zone must be zero:

$$\hat{n} := \{n_x, n_y, n_z\} = \{\cos \chi_n \sin \varphi_n, \sin \chi_n \sin \varphi_n, \cos \varphi_n\}$$

$$\hat{t} := \{t_x, t_y, t_z\} = \{\cos \chi_t \sin \varphi_t, \sin \chi_t \sin \varphi_t, \cos \varphi_t\}$$

$$\hat{n} \bullet \hat{t} = 0 \Leftrightarrow \cos \chi_n \sin\varphi_n \cos \chi_t \sin \varphi_t$$

$$+ \sin \chi_n \sin\varphi_n \sin \chi_t \sin \varphi_t + \cos\varphi_n \cos\varphi_t = 0$$

$$\varphi_n = \tan^{-1} \left\{ \frac{\tan \varphi_t}{\cos \chi_n \cos \chi_t + \sin \chi_n \sin \chi_t} \right\}$$

To use this formula, choose an azimuth angle, ϕ_t, and calculate the declination angle, χ_n, that goes with it.

Effect of Texture:
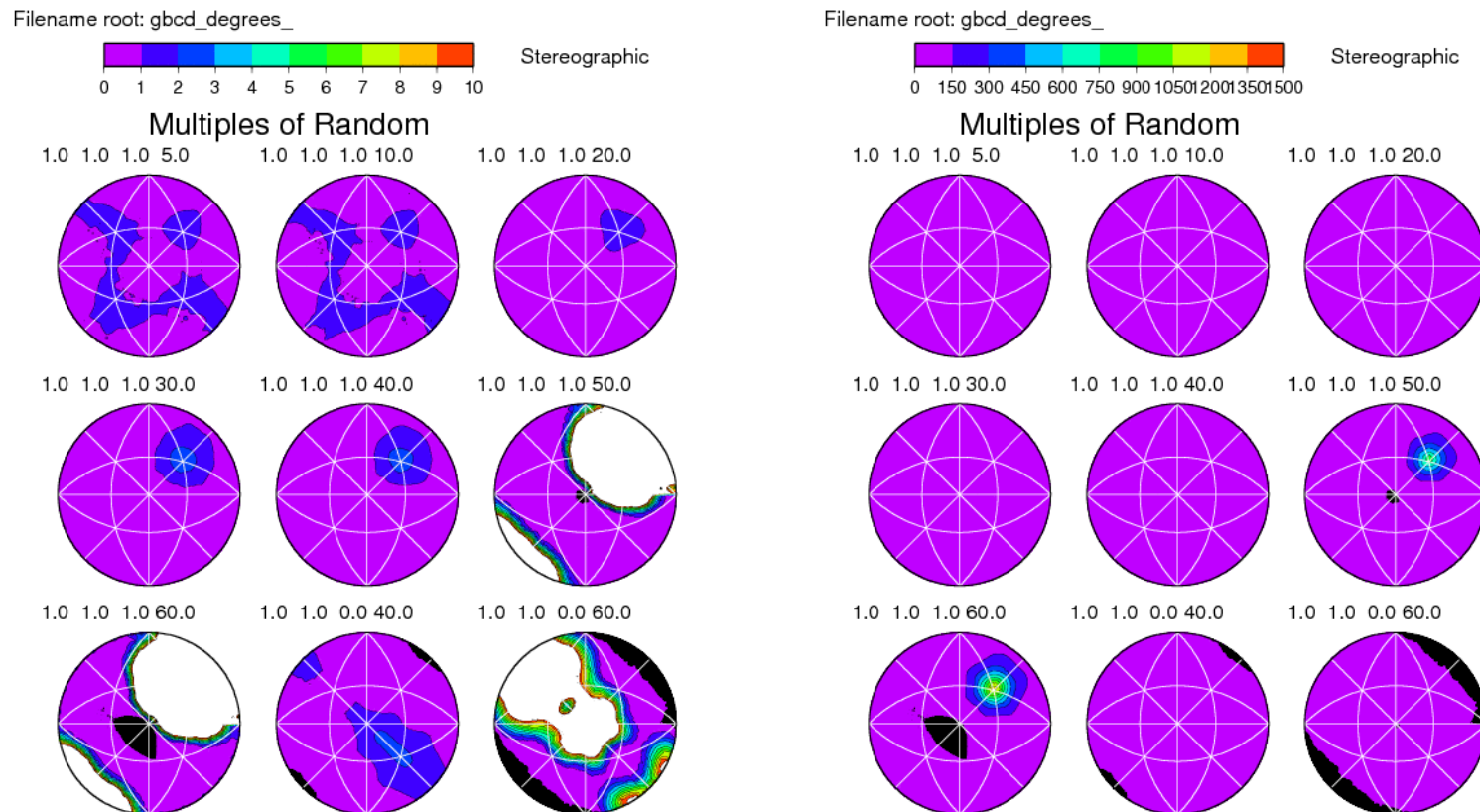# *Distribution of misorientation axes in the sample frame*

- To make a start on the issue of how texture affects stereological measurement of GBCD, consider the distribution of misorientation axes.

- In a uniformly textured material, the misorientation axes are also uniformly (randomly) distributed in sample space.

- In a strongly textured material, this is no longer true, and this perturbs the stereology of the GBCD measurement.

- For example, for a strong fiber texture, e.g. <111>// ND, the misorientation axes are also parallel to the common axis. Therefore the misorientation axes are also //ND. This means that, although all types of tilt and twist boundaries may be present in the material (for an equi-axed grain morphology), all the grain boundaries that one can sample with a section perpendicular to the ND will be much more likely to be tilt boundaries than twist boundaries. This then biases the sampling of the boundaries. In effect, the only boundaries that can be detected are those along the zone of the 111 pole that represents the misorientation axis (see diagram on the right).

(111) Pole

(111) Plane
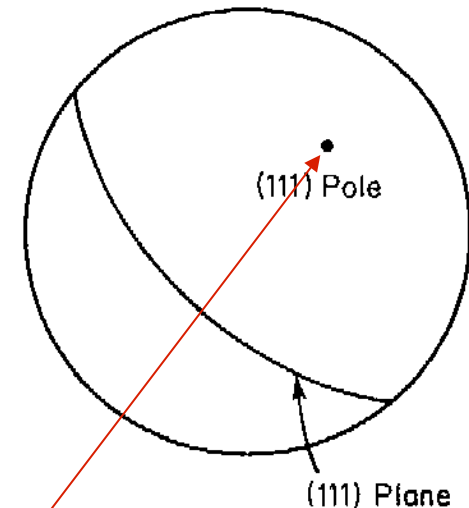
Misorientation axis, e.g. 111

# *GBCD in annealed Ni*

- This Ni sample had a high density of annealing twins, hence an enormous peak for 111/60° twist boundaries (the coherent twin). Two different contour sets shown, with lower values on the left, and higher on the right, because of the variation in frequency of different misorientations.

Misorientation axes: Ni example

- Now we show the distributions of misorientation axes in sample axes, again with lower contour values on the left. Note that for the 111/60° case, the result resembles a pole figure, which of course it is (of selected 111 poles, in this case). The distributions for the 111/60° and the 110/60° cases are surprisingly non-uniform. However, no strong concentration of the misorientation axes exists in a single sample direction.
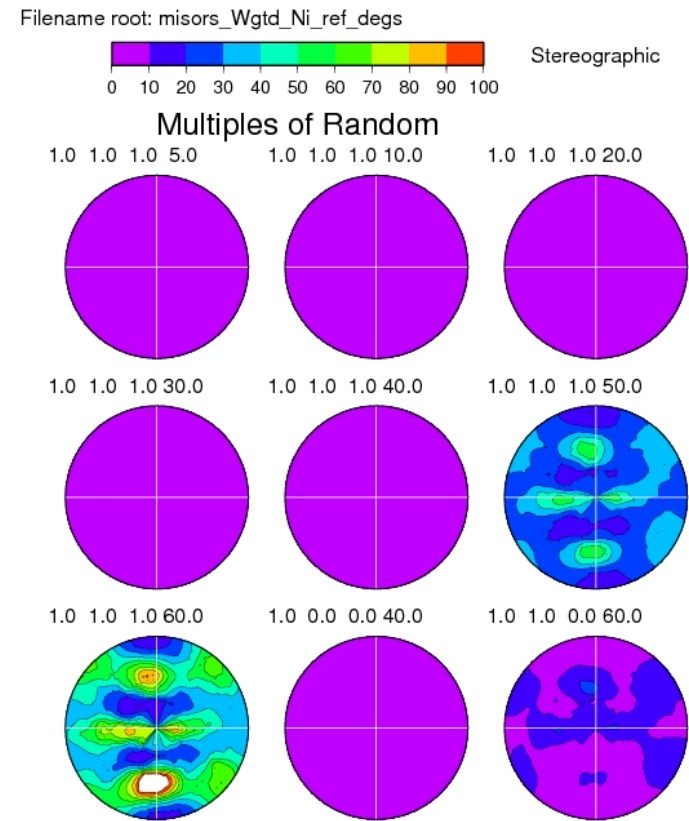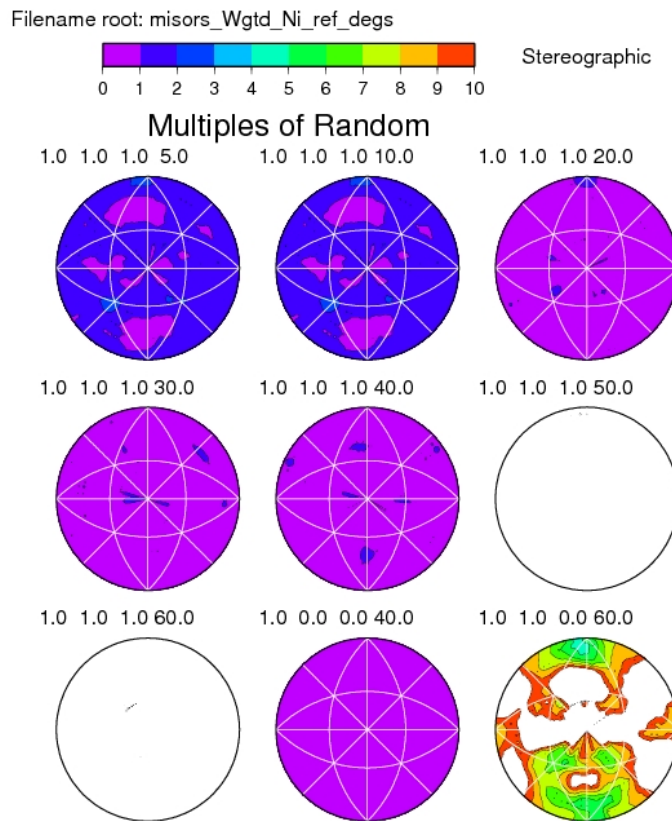
Zones of specimen normals in crystal axes (at each boundary)

- An alternate approach is to consider where the specimen normal lies with respect to the crystal axes, at each grain boundary (and on both sides of the boundary). Rather than drawing/plotting the normal itself, it is better to draw the zone of the normal because this will give information on how uniformly, or otherwise, we are sampling different types of boundaries.

- Note that the crystal frame is chosen so as to fix the misorientation axis in a particular location, just as for the grain boundary character distributions.
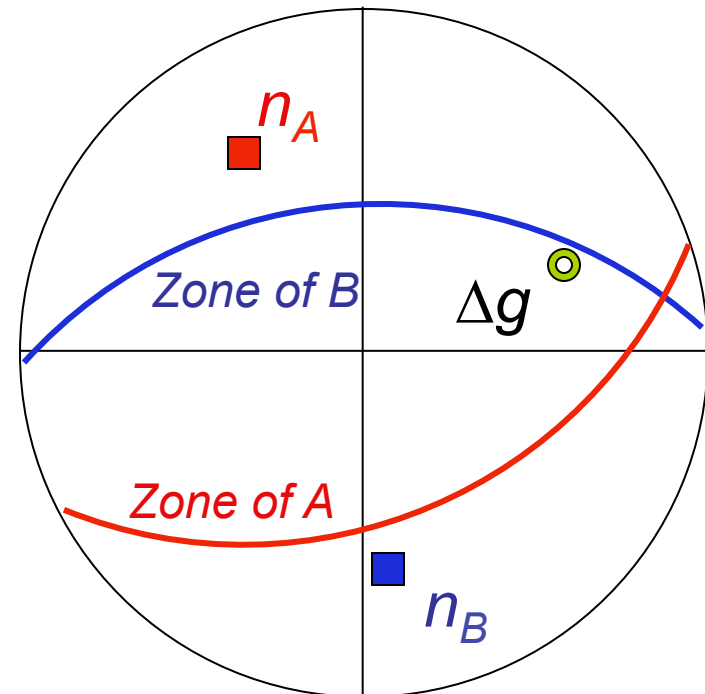
Zones of specimen normals: Ni example

- Again, two different scales to add visualization with lower values on the left. Note that the 111 cases are all quite flat (uniform). The 110/60° case, however, is far from flat, and two of the 3 peaks coincide with the peaks in the GBCD.